Thesis for the Degree of Master of Science

Genetic characteristics and pathogenicity of a novel red sea bream iridovirus mixed subtype I/II in rock bream

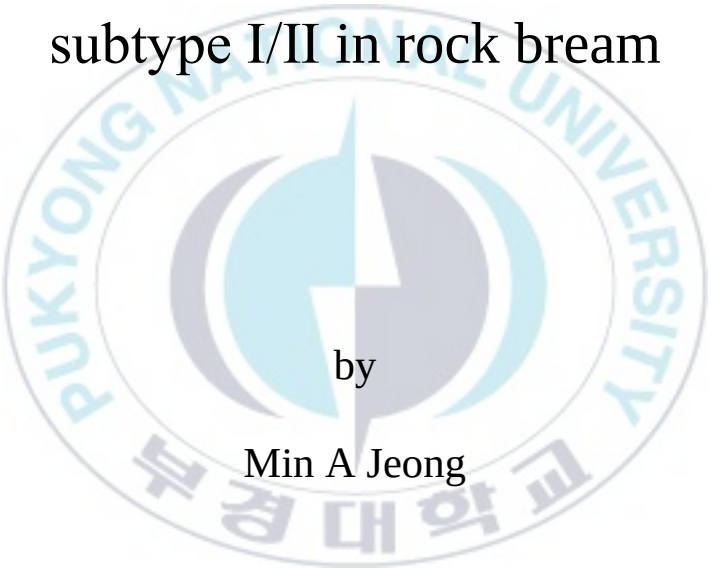

by

Min A Jeong

Department of Aquatic Life Medicine

The Graduate School

Pukyong National University

August 2022

Genetic characteristics and pathogenicity of a novel red sea bream iridovirus mixed subtype I/II in rock bream

(새로운 red sea bream iridovirus mixed subtype I/II 의 유전적 특징과 돌돔에서의 병원성 분석)

Advisor: Prof. Kwang Il Kim

by
Min A Jeong

A thesis submitted in partial fulfilment of the requirements
for the degree of

Master of Science

In the Department of Aquatic Life Medicine, The Graduate School,
Pukyong National University

August 2022

Genetic characteristics and pathogenicity of a novel red sea bream iridovirus mixed subtype I/II in rock bream

A dissertation
by
Min A Jeong

Approved by:

(Chairman) Prof. Ki-Hong Kim

(Member) Prof. Do-Hyung Kim

(Member) Prof. Kwang-Il Kim

August 26, 2022

CONTENTS

새로운 red sea bream iridovirus mixed subtype I/II 의 유전적 특징과 돌돔에서의 병원성 분석

정민아

부경대학교 대학원 수산생명의학과

요약

참돔이리도바이러스병(red sea bream iridoviral disease, RSIVD)의 원인체는 infectious spleen and kidney necrosis virus (ISKNV)와 red sea bream iridovirus (RSIV)로 알려져 있다. 국내에서 1990 년 후반부터 돌돔, 참돔 등의 해산어류에서 RSIVD 발생이 보고되었으며 주 원인체는 RSIV subtype II 형이다. 최근 대만의 양식 참돔에서 ISKNV 와 RSIV 가 혼합된 새로운 변이주인 RSIV-Ku strain 이 확인되어 수계 환경 중 유전자 변이의 가능성이 제시된 바 있다.

본 연구에서는 국내 양식 어류 중 농어(Japanese seabass, *Lateolabrax japonicus*)와 돌돔(Rock bream, *Oplegnathus fasciatus*)에서 RSIV 감염을 확인하였으며, major capsid protein (MCP)와 adenosine triphosphatase (ATPase) 유전자 염기서열을 통한 계통학적 분석 시 다른 유형의 RSIV 인 것을 확인하였다. 서로 다른 유전적 특징을 가지는 RSIV (농어로부터 분리한 subtype I/II 혼합형인 17SbTy 및 돌돔으로부터 분리한

RSIV subtype II)에 대한 차이점을 알고자 전체 게놈을 분석하였으며, 돌돔에 대한 두 분리주의 병원성을 분석하였다. RSIV subtype I/II (17SbTy isolate)와 RSIV subtype II (17RbGs isolate)의 전체 게놈 서열은 각각 112,360, 112,235 bp 길이임을 밝혀냈다. 17SbTy isolate 의 전체 open reading frame (ORF) 115 개 염기서열에 대한 참조 서열들광의 상동성을 분석 한 결과, 69 개의 ORF 는 RSIV subtype II (98.48–100% 상동성), 46 개의 ORF 는 subtype I (98.77–100% 상동성)과 가장 유전적 상동성이 높은 것으로 확인되었다. 또한, 일본에서 보고한 Ehime-1 strain (RSIV subtype I)과 국내 RBIV strain (RBIV subtype II)와 본 연구에서 분리된 RSIV 와의 유전적 변이를 비교하였다. 그 결과 RSIV subtype I/II (17SbTy isolate)와 RSIV subtype II (17RbGs isolate)는 기능성 단백질(DNA-binding protein 과 myristoylated membrane protein)을 암호화하는 영역에서 두 개의 insertion/deletion 변이(17SbTy 기준 ORF 014R 및 102R)를 가지고 있다.

RSIV subtype I/II (17SbTy isolate)와 RSIV subtype II (17RbGs isolate)를 돌돔에 인위 감염 시 감염된 돌돔의 생존률은 그룹 간의 유의적인 차이를 보였다. 이는 게놈 특성 또는 각각의 원래 숙주에 대한 적응이 병원성에 영향을 미칠 수 있음을 나타낸다. 인위 감염된 돌돔의 최대 RSIV shedding ratio 로부터 RSIV 전파에 대한 평가 시 RSIV subtype I/II 감염은 RSIV subtype II 에 비해 상대적으로 낮은 위험성을 보이는 것으로 확인되었다. 또한, 돌돔의 spleen index 수치를 기반으로 두 RSIV 감염에 대한 odds ratio 을 분석 시 RSIV subtype I/II 는 19.38 인 반면 RSIV subtype II 감염 시 55.00 로 유의적인 차이를 보였으며 이는 RSIV 간 돌돔에 대한 병원성 차이를 뒷받침하였다. 특히, 자연 수계 환경 조건을 모방한 cohabitation 감염

실험에서 donor (RSIV 복강 접종 돌돔)와 recipient (donor 와 함께 수용된 돌돔)의 누적 사망률은 RSIV subtype I/II 노출이 RSIV subtype II 노출 그룹에서 유의하게 낮아 유전적 변이와 병원성 간의 상관관계를 뒷받침했다. 유전적 및 돌돔에 대한 병원성 차이를 보이는 두 RSIV 의 돌돔에서의 감염 기작을 확인하고자 각각의 RSIV 를 돌돔에 인위 감염 후 바이러스 자체 및 돌돔의 세포자멸사(apopotosis) 관련된 유전자들의 발현을 분석하였다. 인위감염된 돌돔에서 insertion/deletion 변이 (InDels) 부위인 DNA-binding protein 과 myristoylated membrane protein 과 세포자멸사와 관련된 caspase-8 의 발현은 감염 후 11 일 동안 두 RSIV 분리주 사이의 유의한 차이를 보이며 up-regulation 되었다. 이는 두 분리주의 감염 초기 단계의 바이러스 복제 정도의 차이와 관련될 수 있다. 또한, 초기 감염 단계에서 바이러스 유전자와 caspase-8 의 높은 발현과 달리, caspase-8 에 의해 활성화 되는 caspase-3 의 낮은 발현은 바이러스가 세포자멸사를 억제했을 수 있으며, 이는 서로 다른 RSIV 분리주 사이의 독성 차이를 반영한다.

결론적으로 유전적 특징이 다른 RSIV subtype I/II 과 RSIV subtype II 의 돌돔에 대한 병원성, viral shedding ratios, odds ratio, 유전자 발현을 포함하는 다양한 요소들은 RSIV subtype I/II 혼합형이 자연 수계 환경에서 일반적인 RSIV subtype II 에 비해 비교적으로 병원성 및 전파력이 낮은 형태의 RSIV variants 일 수 있다는 것을 뒷받침한다.

List of Tables

List of Figures

I. Introduction

Red sea bream iridoviral disease (RSIVD) caused by *red sea bream iridovirus* (RSIV) and *infectious spleen and kidney necrosis virus* (ISKNV) (Genus *Megalocytivirus*, family *Iridoviridae*) has to outbreak more than 30 species of freshwater and marine fish species since the 1990s (Chinchar *et al.*, 2017; OIE, 2021). Based on the phylogeny of major capsid protein (MCP) or adenosine triphosphate (ATPase) genes, the isolates can be classified into three major genotypes: RSIV, ISKNV, and turbot reddish body iridovirus (TRBIV) (Kurita and Nakajima, 2012). RSIV and ISKNV can be further classified into two subtypes, respectively (Kurita and Nakajima, 2012). Since the first outbreak of an RSIV (RSIV subtype I) infection to red sea breams (*Pagrus major*) in Japan in 1990 (Inouye *et al.*, 1992), RSIVs have been transmitted through marine fish in East Asian countries (Kim *et al.,* 2019; Kawakami *et al.,* 2002; Jeong *et al.,* 2003). In Korea, rock bream iridovirus (RBIV), which is one of the RSIV subtype II viruses, was identified from rock bream (*Oplegnathus fasciatus*) in 1998 (Jung *et al.,* 2000). RSIV (Kawakami *et al.*, 2002; Jeong *et al.,* 2003; Oh *et al.*, 1999) and TRBIV (Do *et al.,* 2005) types have been reported as endemic in Korea. Especially, RSIV subtype II has been identified as the major causative pathogen of endemic RSIVD in cultured marine fish in Korea (Kim *et al.,* 2019).

In Taiwan, an ISKNV/RSIV recombinant type was isolated from the red sea bream (*Pagrus major*) in 2016 and is known as RSIV-Ku (Shiu *et al.,* 2018). Its genome shares

a high degree of homology with ISKNV-type viruses, except for specific nucleotide sequences that are closely related to RSIV-type viruses (Shiu *et al.*, 2018). Recently, a novel RSIV strain (SB5-TY) from a diseased Japanese seabass (*Lateolabrax japonicus*) in Korea is believed to be a genetic variant of RSIV-type viruses based on sequence difference in MCP and ankyrin repeat domains (Kim *et al.*, 2019). Thus, the emergence of genetic recombinants or variants of *Megalocytivirus* is a possibility, especially in RSIVD-endemic regions, such as Korea. Therefore, complete genome sequence and virulence analyses of isolates in susceptible hosts are crucial for epidemiological studies, such as source tracking and virus transmission studies.

Assessment of the transmission of pathogens could provide pivotal information for understanding their risks in host species (Tompkins *et al.*, 2015; Fusianto *et al.*, 2021). In particular, pathogenic evaluation in the natural environment and/or mimic conditions, such as the cohabitation method, is a reliable assessment of viral transmission in the aquatic environment. Furthermore, evaluation of the viral shedding ratio from infected fish by determining the viral concentration in rearing water can be used to estimate the risk of viral transmission to naïve fish (Go and Whittington, 2019; Min *et al.*, 2021). In a variety of previous studies, although RSIV has been demonstrated to be able to transmit through environmental water as horizontal transmission (He *et al.*, 2002; Kawato *et al.*, 2017), studies on viral shedding are still lacking.

Genetic variation among viral strains and/or isolates can affect their pathogenicity to the host. To explain the relationship between genetic variation and virulence of RSIV isolates, analysis of the viral replication and immune response in the infected host is

needed. In the immune system, the degradation of many cellular proteins by intracellular enzymes, such as caspases (cysteine-aspartic specific proteases), mainly results in apoptosis (Everett *et al.*, 1999; Orzalli and Kagan, 2017). Apoptosis can be induced by two main pathways: the activation of caspase-8 and -9 (Dockrell, 2001). In addition, programmed cell death 10 (PDCD10) plays a role in t inducing apoptosis through the activation of the caspase-3 pathway (Chen *et al.*, 2009; Kim *et al.*, 2016). Among the virulence-related factors of RSIV, caspase-dependent apoptosis induced by RSIV infection can cause host cell death (Imajoh *et al.*, 2004; Jung *et al.*, 2012). Thus, the correlation between viral genes and apoptosis-related gene expression in the RSIV-infected host can be key to elucidating the virulence differences between RSIV isolates.

In the present study, the complete genome sequences of two RSIVs (RSIV mixed subtype I/II and subtywere pe II) were identified from two cultured marine fish species, Japanese seabass (*Lateolabrax japonicus*) and the rock bream (*Oplegnathus fasciatus*), in Korea were determined, and analyzed their insertion/deletion mutations (InDels). In addition, the difference in viral replication in rock bream fin (RBF) cells, mortality in rock bream mimicking natural conditions, and viral shedding ratio between RSIV subtype II and mixed subtype I/II isolates were compared. The virulence of RSIV mixed subtype I/II was determined by viral gene and apoptosis-related gene expression in infected rock bream.

II. Materials and methods

1. Virus culture

RBF cells (Jeong *et al.*, 2021) were propagated at 25 °C in L-15 medium (Gibco, Grand Island, NY, USA) supplemented with 15% fetal bovine serum (FBS, Performance Plus; Gibco, USA), 1% non-essential amino acids, 25 mmol/L HEPES solution, and 1% antibiotic-antimycotic solution (Gibco, USA).

Tissue samples (spleen and kidney, 50 mg) were collected from diseased Japanese seabass in Tongyeong and rock bream in Goseong in 2017. To identify RSIV infection, real-time polymerase chain reaction (qPCR) (Chen *et al.*, 2009) was carried out. Briefly, each 20 μL qPCR mixture contained 1 μL of DNA, which was extracted using the yesG^{TM} Cell Tissue Mini Kit (GensGen, Busan, Korea), 200 nM for each primer and probe (Table 1), 10 μL of the 2× HS Prime qPCR Premix (Genet Bio, Daejeon, Korea), 0.4 μL of the 50× ROX dye, and 5.6 μL of nuclease-free water. Amplification was performed using a StepOne Real-time PCR system (Applied Biosystems, Foster City, CA, USA) under the following conditions: 95 °C for 10 min, followed by 40 cycles of 94 °C for 10 s (denaturation) and 60 °C for 35 s (annealing and extension). Tissue samples that were RSIV-positive, as determined by qPCR, were used as the viral inoculum. Viral infection (each cultured virus, 10^6 viral genome copies/mL) was induced in 75 cm^2 tissue culture flasks (Greiner Bio-one, Frickenhausen, Germany)

containing monolayers (80–90% confluency) of RBF cells (approximately 10^5 cells/mL).

RSIV-infected cells were propagated at 25 °C for seven days in an L-15 medium supplemented with 5% FBS and 1% antibiotic-antimycotic solution. After the appearance of cytopathic effects (rounded cells), infected cells were freeze-thawed thrice. Virus-containing supernatants were collected after centrifugation at 500 ×*g* for 10 min and stored at −80 °C until use. The cultured RSIVs were designated as 17SbTy and 17RbGs based on the sampling year, letters from the common fish name, and the sampling site (i.e., 2017, Japanese seabass, Tongyeong and 2017, rock bream, Goseong). Viral genome copies were determined using qPCR mentioned as above.

Table 1. The PCR and qPCR primers used in this study

Primer	Target	Sequence(5'-3')	Reference
RSIV 1094F RSIV 1221R RSIV 1177 probe	Major capsid protein	CCA GCA TGC CTG AGA TGG A GTC CGA CAC CTT ACA TGA CAG G FAM-TAC GGC CGC CTG TCC AAC G-BHQ1	Kim *et al.*, 2021
1-F 1-R	*Pst* I fragment	CTC AAA CAC TCT GGC TCA TC GCA CCA ACA CAT CTC CTA TC	Kurita *et al.*, 1998
4-F 4-R	DNA polymerase gene	CGG GGG CAA TGA CGA CTA CA CCG CCT GTG CCT TTT CTG GA	
MCP 1F MCP 300R MCP 600F MCP 800R MCP 1015F MCP 1362R	Major capsid protein	ATG TCT GCR ATC TCA GGT GC CCA GCG RAT GTA GCT GTT CTC CAA GCT GCG GCG CTG GGA GG GGC GCC ACC TGR CAC TGY TC CTC ATT TTA CGA GAA CAC CC TYA CAG GAT AGG GAA GCC TGC	Kim *et al.*, 2018
ATPase 1F ATPase 218R ATPase 529F ATPase 721R	ATPase	ATG GAA ATC MAA GAR TTG TCC YTG CAG TTR GGC AAY AGC TTG CT GGG GGY AAC ATA CCM AAG C CTT GCT TAC RCC ACG CCA G	This study

2. Complete genome sequence analysis

2-1. Complete genome sequencing by next-generation sequencing

Viral nucleic acids were extracted from gradient-purified virions using the QIAamp MinElute virus spin kit (Qiagen, Hilden, Germany). Next, 1 μg of the extracted DNA was employed to construct sequencing libraries with the QIAseq FX Single Cell DNA Library Kit (Qiagen, Hilden, Germany). Sequencing libraries of 17SbTy and 17RbGs were constructed, with average lengths of 648 bp and 559 bp, respectively. The quality of the libraries was evaluated using the Agilent High Sensitivity D 500 ScreenTape system (Agilent Scientific, CA, USA), and the quantity was determined by means of a Light Cycler Real-time PCR system (Roche, Mannheim, Germany). The high-quality libraries (300–600 bp) were sequenced (pair-end sequencing, 2 × 150 bp) by G&C Bio Co. (Daejeon, Korea) on the Illumina HiSeq platform (Illumina, CA, USA). To assess the quality of the sequence data, FastQC (Andrews, 2010) and MultiQC (Ewels *et al.*, 2016) were employed. Low-quality sequences (base quality <20) and the Illumina universal adapters were trimmed from the reads in the Trim-Galore software (ver. 0.6.1; https://www.bioinformatic s.babraham.ac.uk/projects/trim_galore). High-quality reads were mapped and assembled into contigs using gsMapper (ver. 2.8). Nucleotide errors in the reads were corrected by means of the Illumina sequence data with the Proovread software (Hackl *et al.*, 2014).

2-2. Circular map

The composition, structure, and homologous regions of the genomic DNA were analyzed using the cgview comparison tool (Grant *et al.*, 2012). A circular map was generated based on the data from the cgview comparison tool. Coding regions were classified according to clusters of orthologous groups (COG) analysis and were denoted as different colours by category. To determine COG categories, a comparative analysis based on the proteins encoded in 43 complete genomes representing 30 major phylogenetic lineages described by Tatusov *et al.* (1997 and 2001) (Tatusov *et al.*, 1997; Tatusov *et al.*, 2001) was performed using the COG program on the National Center for Biotechnology Information (NCBI) website (http://www.ncbi.nlm.nih.gov/COG). And then the genes were categorized in accordance with their functional annotations.

2-3. Gene annotation and open reading frame (ORF) analysis

To identify putative ORFs, the full-length genome sequences of 17SbTy and 17RbGs were annotated in Prokka (ver. 2.1). ORFs were predicted using the NCBI ORF finder (https://www.ncbi.nlm.nih.gov/orffinder), and then the amino acid sequences of the putative ORFs were checked by means of Protein BLAST (BLASTp; https://blast.ncbi.nlm.nih.gov/Blast.cgi). Nucleotide sequence homologies of the putative ORFs of 17SbTy were determined in comparison to those of 17RbGs and representative megalocytiviruses, i.e., Ehime-1 (GenBank accession No. AB104413; RSIV subtype I and the ancestral strain of RSIVD) (Kurita *et al.*, 2002), ISKNV (GenBank accession No. AF371960) (He *et al.*, 2001), and TRBIV (GenBank accession No. GQ273492)] (Shi *et al.*, 2010) using BLAST (https://blast.ncbi.nlm.nih.gov/Blast.cgi). For genotyping, genes encoding MCP and ATPase were amplified with the primers listed in Table 1 and sequenced using an ABI 3730XL DNA Analyzer (Applied Biosystems, CA, USA) by Bionics Co. (Seoul, Korea). Then, the MCP and ATPase gene sequences were quality-checked by base-calling using ChromasPro (ver. 1.7.5; Technelysium, Tewantin, Australia). Each sequence was identified using Nucleotide Basic Local Alignment Search Tool (BLASTn; https://blast.ncbi.nlm.nih.gov/Blast.cgi). Contigs were generated using the ChromasPro and aligned using the ClustalW algorithm in BioEdit (ver. 7.2.5). Phylogenetic trees were generated by the maximum likelihood method via the Kimura two-parameter (K2P) model with a gamma-distribution and invariant sites (K2P + G4

+ I) using MEGA (ver. 11). The MCP and ATPase genes of epizootic haematopoietic necrosis virus (GenBank accession no. FJ433873) were used as outgroup in the phylogenetic analyses. Support for specific genotypes of the RSIVs were determined with 1000 bootstrap replicates (≥70%). Furthermore, to analyze genetic relatedness of viruses in *Iridoviridae*, amino acid sequences of 26 conserved genes (Eaton *et al.*, 2007; Eaton *et al.*, 2010) were retrieved from NCBI GenBank. A phylogenetic tree based on the deduced amino acid sequences of 26 concatenated genes was constructed by the maximum likelihood method via LG model and gamma-distributed with invariant sites (LG + G4 + I) (Do *et al.*, 2004) in MEGA (ver. 11.).

2-4. Analysis of insertion and deletion mutations with RSIVs

To identify InDels in coding regions, the nucleotide sequences of 17SbTy and 17RbGs were compared with those of the ancestral RSIV (Ehime-1 isolated from a red sea bream in Japan in 1990; RSIV subtype I) (Kurita *et al.*, 2002) and an RSIV previously reported in Korea (RBIV-KOR-TY1 isolate found in a rock bream in 2000; RSIV subtype II; GenBank accession No. AY532606) (Do *et al.*, 2004), respectively. Genomic sequences coding for functional proteins were aligned using the ClustalW algorithm in BioEdit (ver. 7.2.), and then InDels were found in the coding regions.

3. Virulence evaluation of red sea bream iridovirus

3-1. Viral replication kinetics on RBF cell (*in vitro*)

To compare the number of viral genome copies in RSIV-infected RBF cells, cultured RSIVs were inoculated into RBF cells and quantitatively analyzed. Approximately 1×10^4 cells per well (500 μL/well) were seeded in 24 cell culture well plates (Greiner Bio-One, Frickenhausen, Germany) and then incubated for 24 h at 25 ℃. Two cultured RSIVs (1×10^6 viral genome copies/mL) were inoculated into the monolayer cells. After absorption for 1 h, each well was washed with phosphate-buffered saline (PBS) and fresh L-15 medium supplemented with 5% FBS and 1% antibiotic-antimycotic solution. RSIV-inoculated cells were incubated for 11 days at 25 ℃. Cell supernatants were collected at 1, 3, 5, 7, 9, and 11 days post-inoculation (dpi) and DNA was extracted using the yesG™ Cell Tissue Mini Cell Tissue Mini Kit (GensGen, Busan, Korea). The number of viral genome copies was determined using qPCR, as described above.

3-2. Experimental fish

Healthy fish (*Oplegnathus fasciatus*; length: 8.75 ± 1.95 cm [mean ± SD], weight: 6.79 ± 4.16 g) were purchased from aquaculture farms in Geoje, Korea. Experimental fish were acclimatized in a circular tank (500 L) at 25.0 ± 0.5 °C for 2 weeks. Each day, fish were fed a commercial diet once a day, and approximately 50% of the rearing water was replaced with temperature-adjusted (25.0 °C) fresh seawater. The experimental fish were confirmed to be RSIV-free for randomly ten rock breams by PCR assay, as described in the Manual of Diagnostic Tests for Aquatic Animals for RSIVD (OIE, 2021; Kurita *et al.*, 1998) and qPCR (Kim *et al.*, 2021). All the animal care and use protocol in this study was reviewed and approved by the institutional animal care and use committee (IACUC) at Pukyong National University (Permission No. PKNUIACUC-2021-33).

3-3. Pathogenicity of RSIVs (*in vivo*)

3-3-1. Pathogenicity of two RSIVs against rock bream

In challenge test, each experimental fish group was intraperitoneally injected (IP) with 0.1 mL of 17SbTy (n = 21; 10^4 viral genome copies per fish), 17RbGs (n = 21; 10^4 viral genome copies per fish), or PBS (n = 21; a negative control). After the viral challenge, the fish were maintained at 25.0 ± 0.5 ℃ in 30 L aqua tanks for 3 weeks, with the 50% water exchange daily. DNA was extracted from the spleen tissue of dead fish, and RSIV infection was confirmed via qPCR. The significance of the difference in the survival rates among the experimental groups was determined by the log-rank test in the GraphPad Prism software (ver. 9.3.1., GraphPad Software Inc.). Data with a P value less than 0.05 were considered significant.

3-3-2. Analysis of odds ratio

To analyze the relative risk of the two RSIV isolates compared to naïve fish, the odds ratio was determined based on the clinical signs (abnormal swimming and lethargy) and spleen index [spleen weight [g] / fish weight [g] × 100] after RSIV infection (performed on the 3-3-1 section). The odds ratio (infected case with clinical sign × uninfected case without clinical sign/infected case without clinical sign × uninfected case with clinical sign) was calculated using the chi-square test with SPSS Statistics 27 (SPSS Inc., Chicago, IL, USA). Statistical significance was set at $P < 0.05$.

3-3-3. Viral shedding ratio

To compare the viral genome copy numbers between the RSIV-infected rock bream and rearing seawater, spleen tissue (n = 3 per sampling day) and rearing water (500 mL) were collected at 1, 3, 5, 7, 9, 11, and 14 days post-injection. RSIV particles in rearing seawater were concentrated using an iron flocculation assay, with some modifications (John *et al.*, 2011; Kawato *et al.*, 2016). Seawater was pre-filtered through a glass microfiber filter (GF/A; pore size, 1.6 μm; Whatman, UK). Next, 50 μL of $FeCl_3$ solution (4.83 g per 100 mL of $FeCl_3 \cdot 6H_2O$ distilled water) was added to pre-filtered seawater (500 mL) and mixed using a magnetic stirrer (< 120 rpm) for 1 h at 20 ℃. The Fe-RSIV flocculate was collected on a polyethylene sulfone membrane (PES; pore size: 0.8 μm; Micron Technology, USA) using a peristaltic pump at < 15 psi (Eyela, Tokyo, Japan). After collecting the Fe-RSIV flocculate, the membrane was transferred to a 5 mL round bottom tube, and 2 mL of elution buffer (0.1M Tris-0.1 M EDTA·$6H_2O$-0.1 M $MgCl_2 \cdot 6H_2O$-0.1 M oxalic acid, pH 6.0) were added. Viral resuspension was performed overnight (approximately 20 h) using a Bio RS-24 Mini-Rotator (30 rpm; Biosan, Riga, Latvia) in a dark room at 4 ℃. The concentration of rearing water in each sample (1, 3, 5, 7, 9, 11, and 14 days post-infection) was measured in triplicates. The number of viral genome copies in the concentrate (viral particles in seawater) and spleen (viral particles in rock bream) were determined by qPCR as described above. To determine the viral shedding ratio from RSIV-infected rock bream (viral genome copies number/L/g), the mean of viral genome copies was divided by the

mean fish weight. The viral shedding ratios from each RSIV-infected rock bream were statistically compared using the two-way ANOVA test in GraphPad Prism (ver. 9.3.1.). Statistical significance was supported by *P*-values (statistical significance was set at $P < 0.05$).

3-4. Cohabitation challenge

To identify viral transmission under natural mimic conditions, the cohabitation method was used. Rock bream (donor, n = 15 in each group) was intraperitoneally injected with diluted RSIV at a high dose (10^4 viral genome copies/100 μL/fish) and low dose (10^2 viral genome copies/100 μL/fish), respectively. RSIV-injected rock bream corresponding to the four groups was cohabitated with naïve fish (recipient, n = 15 in each group). In the negative group, PBS-injected rock bream (n = 15) was cohabitated with naïve fish (n = 15). Rock breams (donor and recipient) were maintained at 25.0 ± 0.5 ℃ in 300 L circular aqua tanks, replacing 50% of rearing seawater daily. After the first death of the donor fish, donor and recipient fish were isolated into 30 L aqua tanks for observing mortality. To identify RSIV infection, DNA was extracted from the spleen tissue of dead and alive fish, and PCR was performed. Mortality rates were compared among the experimental groups using the log-rank test in GraphPad Prism (ver. 9.3.1). Statistical significance was set at $P < 0.05$.

3-5. Expression of viral and apoptosis-related genes

The expression of viral and apoptosis-related genes in rock bream after IP injection of each virus was compared to understand the virulence difference between RSIV isolates. The relative gene expression levels were determined by SYBR-Green based real-time PCR assay, which used template cDNA from the spleen of each triplicate sample (1, 3, 5, 7, 9, and 11 days post-infection), and samples from the control group (PBS) were used as calibrators. To compare viral and apoptosis-related gene expression in the different RSIV-injected rock bream, four viral genes encoding major capsid protein, polymerase, myristoylated membrane protein, and DNA binding protein, and three apoptosis-related genes encoding caspase-3, caspase-8, and PDCD 10 were analyzed. *β-actin* (elongation factor), a housekeeping gene, was used as an endogenous control to normalize the expression value of each target gene. RNA from spleen tissue was extracted using the yesR™ Total RNA extraction kit (GensGen, Korea), followed by cDNA synthesis using a PrimeScript ™ first-strand cDNA synthesis kit (Takara Bio Inc., Japan) according to the manufacturer's instructions. Relative gene expression levels were quantified using the StepOne real-time PCR system (Applied Biosystems, USA). The amplification was performed in a 20 μL final volume containing 1 μL of cDNA sample, 10 μL 2 × Prime Q-Master mix (Genet Bio, South Korea), 0.4 μL 50× ROX dye, 1 μL forward, reverse primer (10 mM; Table 2) and 6.6 μL nuclease-free distilled water. Each SYBR-Green based real-time PCR amplification was performed in duplicate wells using the following SYBR-Green based real-time PCR cycling

conditions: 10 min at 95 °C, followed by a total of 10 s at 95 °C, 40 cycles of 60 °C for 15 s, and 72 °C for 20 s. The melting curve was constructed in the temperature range of 60–95 °C. The relative quantitation value of amplified genes was expressed as $-\Delta\Delta$Ct (fold), calculated by the comparative Ct method. The ΔCt value is the average target gene Ct subtracted from the average β-actin Ct value [ΔCt = average Ct of samples for target gene - average Ct of samples for β-actin], and the -ΔΔCt (units of fold increase over the PBS-injected control fish group) for target gene is the ΔCt of the control group subtracted from the ΔCt of samples [ΔΔCt = ΔCt of samples for target gene - ΔCt of the calibrator for target gene]. The statistical support for relative gene expression between RSIV isolates was determined by a two-way ANOVA test using GraphPad Prism software (ver. 9.3.1.). Statistical significance was set at $P < 0.05$.

Table 2. The SYBR-Green based real-time PCR primers used in this study

Primer	Target	Sequence(5'-3')	Reference
RbEF-1a F RbEF-1a R	Elongation factor (β-actin)	CAG GGA GAA GAT GAC CCA GA CAT AGA TGG GCA CTG TGT GG	Hong *et al.*, 2016
qM1F qM1R	Major capsid protein	GGC GAC TAC CTC ATT AAT GT CCA CCA GGT CGT TAA ATG A	Jin *et al.*, 2018
qPoly1F qPoly1R	Polymerase gene	GTT TAT GGC GGG GGC AAT TGG CCC AGC TGT ATG TAG C	This study
RSIV MyristM F RSIV MyristM R	Myristoyolated membrane protein gene	CGC AGG TAG ACC GCT CCG CCC GCA CGC CGT TGT TCA	This study
RSIV DNABind F RSIV DNABind R	DNA binding protein gene	GGC CTG TCG CAT GTG AGG AG TGC AGG AGT GAC TGC CGC	This study
RbPDCD10F RbPDCD10R	PDCD10	GAA TAG ACG GGT GCT GGA AA TCA TGT TGG TTT GGT GGA TG	Kim *et al.*, 2016
Rbcaspase3F Rbcaspase3R	Caspase 3	TGA GGG TGT GTT CTT TGG TAC GGA TTC CCA CTA GTG ACT TGC AGC GAT	Elvitigala *et al.*, 2012
Rbcaspase8F Rbcaspase8R	Caspase 8	TGA TGA GGT CTG CAC AAA GC TTG AGG ACG AGC TTC TTG GT	Jung *et al.*, 2014

III. Results

1. Characteristics of ~~the~~ RSIV isolates complete genome

1-1. Circular map

The complete genomes of 17SbTy (GenBank accession No. OK042108), and 17RbGs (GenBank accession No. OK042109) comprise 122,360 and 122,235 bp in size. The sequences were circularly permuted and assembled into a circular form (Figure1). In addition, the G+C content was found to be 53.28% and 53.13% in 17SbTy and 17RbGs, respectively.

Of the 26 functional categories identified in the COG analysis, total of 20 protein-coding genes in both 17SbTy (17.39%; 20/115 ORFs) and 17RbGs (17.54%; 20/114 ORFs) were found to be annotated in the COG database (Figure 1; Table 3).

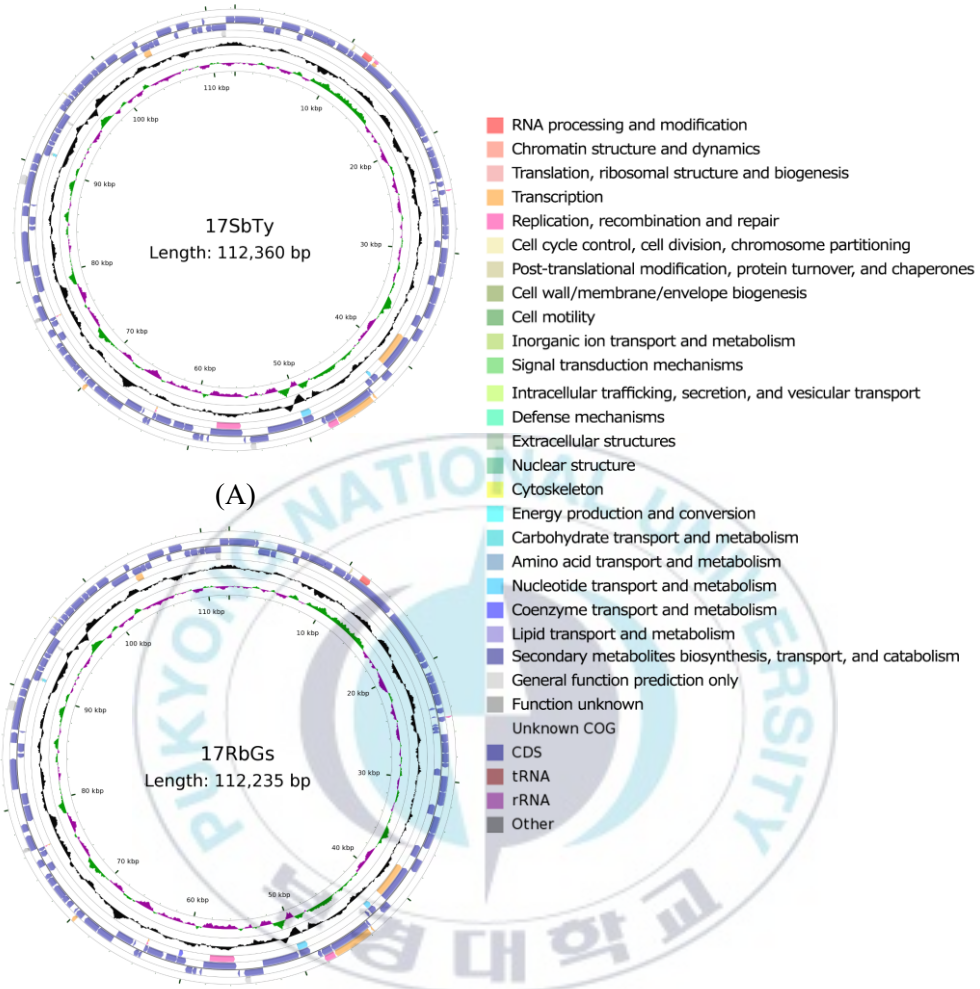

Figure 1. Circular genome maps of (a) 17SbTy (112,360 bp) and (b) 17RbGs (112,235 bp). From the inner ring toward the outer ring, the first and eighth circles represented the genomic length (kbp) and nucleotide positions, respectively. The second and third circles show a G+C skew and G+C content, respectively. The fourth and fifth circles represent rRNA and tRNA genes on forward and reverse strands, respectively. The sixth and seventh circles indicate the functional categories of the protein-coding sequences in terms of clusters of orthologous groups (COG) on the forward and reverse strands, respectively.

Table 3. The coding sequences (CDSs) determined via COG classification of 17SbTy and 17RbGs in four functional categories

No.	Category	COG function	COG description	17SbTy	17RbGS
1	Metabolism	Amino acid transport metabolism	quinoprotein dehydrogenase-associated putative ABC transporter substrate-binding protein	ORF 093L	ORF 092L
2		Nucleotide transport and metabolism	deoxynucleoside kinase	ORF 042L	ORF 041L
3			ribonucleoside-diphosphate reductase	ORF 048L	ORF 047L
4			HIT domain-containing protein	ORF 089L	ORF 088L
5	Information storage and processing	Translation, ribosomal structure and biogenesis	O-acetyl-ADP-ribose deacetylase	ORF 050R	ORF 049R
6		Transcription	DNA-directed RNA polymerase subunit B	ORF 040L	ORF 039L
7			transcription factor S	ORF 044R	ORF 043R
8			DNA-directed RNA polymerase subunit A&apos	ORF 045R	ORF 044R
9			phosphoprotein phosphatase	ORF 066R	ORF 065R
10			ribonuclease III	ORF 105L	ORF 104L
11		Replication, recombination and repair	DNA cytosine methyltransferase	ORF 028R	ORF 027R
12			flap endonuclease-1	ORF 046R	ORF 045R
13			DNA polymerase elongation subunit	ORF 052L	ORF 051L
14	Cellular process	Signal transduction mechanisms	protein-tyrosine-phosphatase	ORF 12R	ORF 012R
15			ankyrin repeat-containing protein	ORF 077R	ORF 076R
16			quinoprotein dehydrogenase-associated putative ABC transporter substrate-binding protein	ORF 093L	ORF 092L
17			ankyrin repeat-containing protein	ORF 115L	ORF 114L
18		Mobilome; prophages, transposons	hypothetical protein	ORF 086R	ORF 085R
19	Poorly characterized	General function prediction only	HIT domain-containing protein	ORF 089L	ORF 088L
20		Function unknown	hypothetical protein	ORF 013R	ORF 012R

1-2. Genomic comparison between RSIVs and other megalocytiviruses

The annotation predicted 115 and 114 putative ORFs in 17SbTy and 17RbGs, respectively (Table 4). The putative ORFs of 17SbTy (total length 104,868 bp, 93.3% of the genome) were found to range in size from 111 to 3,849 bp and to encode 36 to 1,282 amino acid residues. Of the 115 ORFs, 70 are located on the sense (R) strand, and 45 were on the anti-sense (L) strand (Table 4). The putative ORFs of 17RbGs (total length 105,003 bp, 93.6% of genome) range in size from 111 to 4,155 bp, coding for 36 to 1,384 amino acid residues. Of the 114 ORFs, 68 are located on the R strand and 46 were on the L strand. Of the annotated ORFs in 17SbTy (115 ORFs) and 17RbGs (114 ORFs), respectively 43 (37.7%) and 42 (36.8%) could be assigned to a predicted structure and/or functional protein. Of the annotated ORFs in 17SbTy (115 ORFs) and 17RbGs (114 ORFs), respectively 43 (37.7%) and 42 (36.8%) could be assigned to a predicted structure and/or functional protein. The complete nucleotide sequences of 17SbTy and 17RbGs turned out to be closely related to rock bream iridovirus-C1 (RBIV-C1, GenBank accession No. KC244182) with 99.56% and 99.69% identity, respectively. A comparison of the complete nucleotide sequences of 17SbTy and 17RbGs revealed 97.69% identity. In the ORFs of 17SbTy, nucleotide sequence identity with Ehime-1 (RSIV subtype I) proved to be 87.99–100%, with 17RbGs (RSIV subtype II): 88.22–100%, with ISKNV: 86.07–97.58%, and with TRBIV: 80.25–99.66% (Table 4). Notably, the best matches for the nucleotide sequences of the 115 ORFs of

17SbTy were RSIV subtype II viruses (97.48–100% identity in 69 ORFs) and RSIV subtype I viruses (98.77–100% identity in 46 ORFs).

According to the phylogeny of genes of MCP and ATPase, 17RbGs belong to RSIV subtype II. Of note, 17SbTy is grouped with either subtype I or II of RSIV depending on gene used for the phylogenetic analysis: MCP or ATPase, respectively (Figure 2). A comparison of 17SbTy with Ehime-1 (ancestral RSIV subtype I) and 17RbGs (RSIV subtype II), showed 99.63% and 98.24% identity to the MCP gene and 99.03% and 100% identity to the ATPase gene, respectively. Furthermore, both 17SbTy and 17RbGs were found to harbor the 26 conserved genes that were shared by all members of the family *Iridoviridae*. The ORFs corresponding to these 26 core genes are listed in Table 5. The phylogenetic tree based on the concatenated amino acid sequences of the 26 conserved genes revealed that 17SbTy and 17RbGs is grouped with the genus *Megalocytivirus* (Figure 3).

Table 4. Predicted ORFs based on a comparison of isolates 17SbTy to 17RbGs and representative ISKNVs

Gene ID 17SbTy	Position		CDS size (NT)	Predicted structure and/or function	best-match homolog			Homolog to 17RbGs		Homolog to Ehime_1 (AB104413.1)		Homolog to ISKNV (AF371960)		Homolog to TRBIV (GQ273492)	
	Start	End			Genotype	Isolates	Identity (%)	ORF no.	Identity (%)	ORF no.	Identity (%)	ORF no.	Identity (%)	ORF no.	Identity (%)
ORF 001R	111584	2196	2973	hypothetical protein [2]	RSIV subtype II	RSIV KagYT-96 RSIV RIE12-1 GSIV-K1 OSGIV	99.70%	ORF 001R	99.70%	ORF 639R	98.18%	76L	93.44%	69L	92.91%
ORF 002R	2198	2467	270	hypothetical protein	RSIV subtype I	PIV2016 PIV2014a PIV2010 LYCIV RSIV Ehime-1	100.00%	ORF 002R	96.67%	ORF 010R	100.00%	75L	91.30%	68L	87.26%
ORF 003L	2476	3495	1020	hypothetical protein	RSIV subtype I	PIV2016 PIV2014a PIV2010 LYCIV RSIV Ehime-1	100.00%	ORF 003L	98.53%	ORF 016L	100.00%	74R	93.63%	67R	93.94%
ORF 004L	3544	4032	489	hypothetical protein	RSIV subtype I	PIV2016 PIV2014a PIV2010 LYCIV Zhoushan RSIV Ehime-1 LYCIV	100.00%	ORF 004L	95.09%	ORF 019L	100.00%	73R	90.24%	[1] 66R	84.72%
ORF 005R	4015	5625	1611	hypothetical protein	RSIV subtype I	PIV2014a PIV2010 LYCIV Zhoushan RSIV Ehime-1	100.00%	ORF 005R	98.08%	ORF 018R	100.00%	71L	93.61%	65L	93.42%
ORF 006L	5528	6043	516	hypothetical protein	RSIV subtype I	PIV2014a PIV2010 LYCIV Zhoushan RSIV Ehime-1	100.00%	ORF 006L	97.29%	ORF 026R	100.00%	70L	95.20%	-	-
ORF 007R	6065	6796	732	hypothetical protein	RSIV subtype I	PIV2016 PIV2014a PIV2010 LYCIV Zhoushan RSIV Ehime-1	100.00%	ORF 007R	96.86%	ORF 029R	100.00%	69L	86.07%	64L	-
ORF 008R	6808	8241	1434	hypothetical protein	RSIV subtype I	PIV2016 PIV2014a PIV2010 LYCIV Zhoushan RSIV Ehime-1	100.00%	ORF 008R	97.63%	ORF 033R	100.00%	68L	93.58%	63L	88.95%
ORF 009R	8192	8860	669	hypothetical protein	RSIV subtype I	LYCIV Zhoushan	100.00%	ORF 009R	98.06%	ORF 037R	98.80%	67L	90.69%	62L	91.68%
ORF 010R	9087	10130	1044	hypothetical protein	RSIV subtype II / ISKNV subtype I	RSIV KagYT-96 RSIV RIE12-1 GSIV-K1 RSIV-Ku LYCIV Zhoushan OSGIV	100.00%	ORF 010R	99.81%	ORF 042R	98.46%	66L	92.82%	61L	92.53%

ORF 011R	10181	10651	471	RING-finger-containing E3 ubiquitin ligase	RSIV subtype II	RSIV KagYT-96 RSIV RIE12-1 RBIV-C1 LYCIV Zhoushan RSIV_121 17RbGs	100.00%	ORF 011R	100.00%	ORF 049R	98.51%	65L	91.30%	60L	89.17%
ORF 012R	10693	12165	1473	mRNA capping enzyme	RSIV subtype II / ISKNV subtype I	RSIV KagYT-96 RSIV RIE12-1 GSIV-K1 RSIV-Ku LYCIV Zhoushan OSGIV	100.00%	ORF 012R	99.93%	MCE	97.49%	64L	93.36%	59L	93.28%
ORF 013R	12205	14853	2649	putative NTPasel[2]	RSIV subtype II	RSIV KagYT-96 RSIV RIE12-1 GSIV-K1	99.96%	-	-	NTPase	97.92%	63L	93.36%	58L	93.42%
ORF 014R	15174	19067	3849	DNA-binding protein	RSIV subtype II	RSIV KagYT-96 RSIV RIE12-1	100.00%	ORF 013R	99.48%	ORF 077R	96.78%	62L	91.81%	57L	93.08%
ORF 015R	19064	19870	807	putative replication factor and/or DNA binding-packing [2]	RSIV subtype II	RSIV KagYT-96 RSIV RIE12-1 GSIV-K1 RBIV-C1 RSIV_121 OSGIV	100.00%	ORF 014R	92.94%	ORF 092R	97.65%	61L	93.80%	56L	93.06%
ORF 016R	19934	20446	513	hypothetical protein	RSIV subtype II	RSIV KagYT-96 GSIV-K1 OSGIV	100.00%	ORF 015R	89.35%	ORF 097R	96.30%	59L	92.84%	55L	88.95%
ORF 017R	20918	21178	261	hypothetical protein	RSIV subtype II	RSIV KagYT-96 RSIV RIE12-1 SKIV RBIV-C1 RSIV_121 RBIV-KOR-TY1 OSGIV	100.00%	ORF 016R	95.40%	ORF 099R	98.08%	57L	96.17%	54L	95.40%
ORF 018R	21185	21832	648	helicase family [2]	RSIV subtype II	RSIV KagYT-96 GSIV-K1 OSGIV	100.00%	ORF 017R	99.23%	ORF 101R	99.23%	56L	97.22%	53L	97.38%
ORF 019R	21843	22784	942	Serine-threonine protein kina [2]	RSIV subtype II	RSIV KagYT-96 RSIV RIE12-1 GSIV-K1 SKIV RBIV-C1 RSIV_121 OSGIV 17RbGs	100.00%	ORF 018R	100.00%	ORF 106R	96.92%	55L	90.98%	52L	89.81%
ORF 020R	22807	23751	945	hypothetical protein	RSIV subtype II	RSIV KagYT-96 GSIV-K1 SKIV RBIV-C1 RSIV_121 OSGIV 17RbGs	100.00%	ORF 019R	100.00%	ORF 111R	97.67%	54L	90.08%	51L	90.48%
ORF 021L	23785	23979	195	hypothetical protein	RSIV subtype II	RSIV KagYT-96RSIV RIE12-1GSIV-K1SKIVRBIV-	100.00%	ORF 020L	100.00%	ORF 121L	96.91%	53R	91.24%	50R	-

						C1RSIV_121OSGIV17RbGs									
ORF 022R	23981	24433	453	hypothetical protein	RSIV subtype II	RSIV KagYT-96 RSIV RIE12-1 GSIV-K1 SKIV RBIV-C1 RSIV_121 OSGIV 17RbGs	100.00%	ORF 021R	100.00%	ORF 122R	96.47%	52L	88.91%	49L	88.21%
ORF 023L	24522	24657	111	hypothetical protein	RSIV subtype II	RSIV KagYT-96 RSIV RIE12-1 GSIV-K1 SKIV RBIV-C1 RSIV_121 RBIV-KOR-TY1 OSGIV 17RbGs	100.00%	ORF 022L	100.00%	ORF 127L	93.86%	51R	91.46%	-	-
ORF 024R	24712	25140	429	hypothetical protein	RSIV subtype II	RSIV KagYT-96 RSIV RIE12-1 GSIV-K1 RBIV-KOR-TY1 OSGIV	100.00%	ORF 023R	99.77%	ORF 128R	98.37%	50L	93.24%	48L	91.61%
ORF 025L	25208	25378	171	hypothetical protein	RSIV subtype II	RSIV KagYT-96 RSIV RIE12-1 GSIV-K1 SKIV RBIV-C1 RSIV_121 RBIV-KOR-TY1 OSGIV 17RbGs	100.00%	ORF 024L	100.00%	ORF 134L	97.66%	49R	94.74%	-	-
ORF 026L	25394	25747	354	PDGF/VEGF-like protein ORF 135L	RSIV subtype II	RSIV KagYT-96 RSIV RIE12-1 GSIV-K1 OSGIV	100.00%	ORF 025L	99.72%	ORF 135L	97.74%	48R	86.16%	47R	87.39%
ORF 027L	25744	26007	264	hypothetical protein	RSIV subtype II	RSIV KagYT-96 RSIV RIE12-1 GSIV-K1 SKIV RBIV-C1 RSIV_121 RBIV-KOR-TY1 OSGIV 17RbGs	100.00%	ORF 026L	100.00%	ORF 138L	97.35%	47R	93.18%	46R	93.56%
ORF 028R	26167	26850	684	cytosine DNA methyltransferase	RSIV subtype I	PIV2014a PIV2010 LYCIV Zhoushan RSIV Ehime-1	99.85%	ORF 027R	97.95%	ORF 140R	99.85%	46L	94.74%	45L	94.88%
ORF 029R	26844	27758	915	hypothetical protein	RSIV subtype I	PIV2016 PIV2014a PIV2010	100.00%	ORF 028R	96.17%	ORF 145R	100.00%	45L	88.74%	44L	89.84%

						LYCIV Zhoushan RSIV Ehime-1									
ORF 030R	27763	28563	801	hypothetical protein	RSIV subtype I	LYCIV Zhoushan RSIV Ehime-1	100.00%	ORF 029R	97.50%	ORF 151R	100.00%	44L	90.02%	43L	89.51%
ORF 031R	28570	28932	363	Erv1/Alr family [2]	RSIV subtype I	PIV2016 PIV2014a PIV2010 LYCIV Zhoushan RSIV Ehime-1	100.00%	ORF 030R	97.80%	ORF 156R	100.00%	43L	94.21%	42L	95.04%
ORF 032L	29016	29615	600	hypothetical protein	RSIV subtype I	PIV2010 LYCIV Zhoushan RSIV Ehime-1	100.00%	ORF 031L	96.83%	ORF 161L	100.00%	42R	89.33%	41R	91.01%
ORF 033R	29630	30979	1350	hypothetical protein	RSIV subtype I	LYCIV Zhoushan	100.00%	ORF 032R	97.04%	ORF 162R	99.56%	41L	88.96%	40L	90.53%
ORF 034R	30981	32129	1149	hypothetical protein	RSIV subtype I	LYCIV Zhoushan	100.00%	ORF 033R	91.91%	ORF 171R	91.22%	40L	89.65%	39L	98.43%
ORF 035L	32122	33000	879	hypothetical protein	RSIV subtype I	LYCIV Zhoushan RSIV Ehime-1 LYCIV	100.00%	ORF 034L	93.97%	ORF 179L	100.00%	39R	90.22%	38R	90.90%
ORF 036R	33066	34505	1440	hypothetical protein	RSIV subtype I	PIV2016 PIV2014a PIV2010 RSIV Ehime-1	100.00%	ORF 035R	93.75%	ORF 180R	100.00%	38L	90.71%	37L	90.90%
ORF 037R	34514	35863	1350	hypothetical protein	RSIV subtype I	PIV2016 PIV2014a PIV2010 LYCIV Zhoushan RSIV Ehime-1	99.93%	ORF 036R	93.85%	ORF 186R	99.93%	37L	90.11%	36L	90.96%
ORF 038L	35860	36915	1056	hypothetical protein	RSIV subtype I	PIV2010 LYCIV Zhoushan RSIV Ehime-1 LYCIV	100.00%	ORF 037L	95.17%	ORF 197L	100.00%	36R	91.49%	35R	88.93%
ORF 039R	36909	38048	1140	hypothetical protein	RSIV subtype I	PIV2010 LYCIV Zhoushan	100.00%	ORF 038R	95.53%	ORF 198R	99.91%	35L	88.64%	34L	88.88%
ORF 040L	38121	41279	3159	DNA dependent RNA polymerase second largest subunit [2]	RSIV subtype I	LYCIV Zhoushan	100.00%	ORF 039L	96.52%	RPO-2	98.54%	34R	93.78%	33R	94.98%
ORF 041R	41362	42264	903	hypothetical protein	RSIV subtype I	LYCIV Zhoushan	100.00%	ORF 040R	95.90%	ORF 226R	97.79%	33L	91.36%	32L	92.59%
ORF 042L	42327	42943	582	deoxyribonucleoside kinase [2]	RSIV subtype I	LYCIV Zhoushan	100.00%	ORF 041L	88.87%	TK	87.99%	32R	92.16%	31R	99.66%
ORF 043L	43008	43535	243	hypothetical protein	RSIV subtype I	PIV2016 PIV2014a PIV2010 RSIV Ehime-1	98.77%	ORF 042L	95.47%	ORF 237L	98.77%	31.5L	88.89%	30R	93.42%
ORF 044R	43603	43824	222	transcription elongation factor TFIIS [2]	RSIV subtype I	PIV2016PIV2014aPIV2 010LYCIV ZhoushanRSIV Ehime-1	100.00%	ORF 043R	98.20%	ORF 238R	100.00%	29L	96.40%	29L	97.06%
ORF 045R	43831	47337	3507	DNA dependent RNA polymerase largest subunit [2]	RSIV subtype I	LYCIV Zhoushan PIV2016 PIV2014a PIV2010	99.94%	ORF 044R	97.69%	RPO-1	99.37%	28L	94.66%	28L	95.30%

ORF 046R	47354	48250	897	probable XPG/RAD2 type nuclease [2]	RSIV subtype I	PIV2016 PIV2014a PIV2010 LYCIV Zhoushan RSIV Ehime-1	100.00%	ORF 045R	98.33%	ORF 256R	100.00%	27L	96.10%	27L	95.21%
ORF 047R	48272	48595	324	hypothetical protein	RSIV subtype I	PIV2016 PIV2014a PIV2010 LYCIV Zhoushan RSIV Ehime-1	100.00%	ORF 046R	97.53%	ORF 261R	100.00%	26L	92.00%	26L	90.43%
ORF 048L	49064	50002	939	ribonucleotide diphosphate reductase small subunit [2]	RSIV subtype I	PIV2016 PIV2014a PIV2010 RSIV Ehime-1	100.00%	ORF 047L	98.08%	RR-2	100.00%	24R	94.68%	25R	95.21%
ORF 049L	50114	53266	3153	laminin-type epidermal growth factor	RSIV subtype I	PIV2010 RSIV Ehime-1	100.00%	ORF 048L	93.77%	ORF 291L	100.00%	23R	87.35%	24R	88.96%
ORF 050R	53339	54934	1596	LRP16 like protein macro domain-containing protein	RSIV subtype I	PIV2016 PIV2014a PIV2010 RSIV Ehime-1	100.00%	ORF 049R	95.60%	ORF 292R	100.00%	22L	93.41%	23L	93.52%
ORF 051R	55282	55464	183	hypothetical protein	RSIV subtype I	PIV2016 PIV2014a PIV2010 LYCIV Zhoushan RSIV Ehime-1 LYCIV	100.00%	ORF 050R	97.27%	ORF 300R	100.00%	20L	89.95%	21L	94.54%
ORF 052L	55511	58354	2844	DNA polymerase family B exonuclease[2]	RSIV subtype I	PIV2010 LYCIV Zhoushan RSIV Ehime-1	100.00%	ORF 051L	97.23%	DPO	100.00%	19R	95.11%	20R	93.15%
ORF 053R	58420	58629	210	hypothetical protein	RSIV subtype I	PIV2010 LYCIV Zhoushan RSIV Ehime-1	100.00%	ORF 052R	92.55%	ORF 318R	100.00%	18.5L	89.89%	19L	91.76%
ORF 054R	58889	59221	333	hypothetical protein	RSIV subtype I	PIV2016 PIV2014a PIV2010 LYCIV Zhoushan RSIV Ehime-1	100.00%	ORF 053R	88.22%	ORF 321R	100.00%	17L	92.81%	17L	89.47%
ORF 055R	59236	59823	588	hypothetical protein	RSIV subtype I	PIV2016 PIV2014a PIV2010 LYCIV Zhoushan RSIV Ehime-1	99.66%	ORF 054R	92.35%	ORF 324R	99.66%	16L	91.50%	16L	92.35%
ORF 056L	59881	60672	792	hypothetical protein	RSIV subtype II	RSIV KagYT-96 RSIV RIE12-1 GSIV-K1 LYCIV Zhoushan RBIV-KOR-TY1 OSGIV	92.12%	ORF 055L	95.58%	ORF 333L	98.86%	15R	94.44%	15R	93.43%
ORF 057L	60678	61652	975	hypothetical protein	RSIV subtype II	RSIV KagYT-96 RSIV RIE12-1 GSIV-K1 LYCIV Zhoushan OSGIV	100.00%	ORF 056L	99.90%	ORF 342L	97.03%	14R	92.31%	14R	92.23%

ORF 058L	61907	63304	1398	serine/threonine protein kinase [2]	RSIV subtype II	RSIV KagYT-96 RSIV RIE12-1 OSGIV	100.00%	ORF 057L	99.93%	ORF 349L	97.49%	13R	90.19%	13R	91.91%
ORF 059L	63311	63643	333	RING-finger-containing ubiquitin ligase	RSIV subtype II	RSIV KagYT-96 RSIV RIE12-1 GSIV-K1 RBIV-C1 LYCIV Zhoushan RSIV_121 RBIV-KOR-TY1 OSGIV 17RbGs	100.00%	ORF 058L	100.00%	ORF 350L	98.50%	12R	96.36%	12R	95.80%
ORF 060R	63662	63922	261	hypothetical protein	RSIV subtype II	RSIV KagYT-96 RSIV RIE12-1 GSIV-K1 RBIV-C1 LYCIV Zhoushan RSIV_121 OSGIV	100.00%	ORF 059R	98.04%	ORF 351R	96.55%	11L	95.02%	11L	94.90%
ORF 061R	63919	64311	393	hypothetical protein	RSIV subtype II	RSIV KagYT-96 RSIV RIE12-1 RBIV-C1 RSIV_121 RBIV-KOR-TY1	100.00%	ORF 060R	92.11%	ORF 353R	97.96%	10L	92.62%	10L	92.11%
ORF 062L	64470	64631	162	hypothetical protein	RSIV subtype II	RSIV KagYT-96 RSIV RIE12-1 GSIV-K1 RBIV-C1 LYCIV Zhoushan RSIV_121 RBIV-KOR-TY1 OSGIV 17RbGs	100.00%	ORF 061L	100.00%	ORF 360L	98.77%	9R	97.53%	9R	98.77%
ORF 063L	64727	66274	1548	hypothetical protein	RSIV subtype II	RSIV KagYT-96 RSIV RIE12-1 GSIV-K1 RBIV-C1 LYCIV Zhoushan RSIV_121 OSGIV 17RbGs	100.00%	ORF 062L	100.00%	ORF 373L	96.13%	8R	91.88%	8R	91.68%
ORF 064R	66345	67802	1458	myristoylated membrane protein [2]	RSIV subtype II	RSIV KagYT-96RSIV RIE12-1GSIV-K1LYCIV ZhoushanOSGIV	100.00%	ORF 063R	99.73%	ORF 374R	97.46%	7L	94.51%	7L	94.65%
ORF 065R	67819	69180	1362	major capsid protein [2]	RSIV subtype I	LYCIV Zhoushan	100.00%	ORF 064R	98.24%	MCP	99.63%	6L	94.57%	6L	94.27%
ORF 066R	69326	70090	765	NIF-NLI interacting factor-like phosphatase [2]	RSIV subtype I	PIV2016 PIV2014a PIV2010 LYCIV Zhoushan RSIV Ehime-1 LYCIV	100.00%	ORF 065R	98.35%	ORF 385R	100.00%	5L	95.17%	5L	92.82%

ORF 067R	70164	70340	177	hypothetical protein	RSIV subtype I	PIV2016 PIV2014a PIV2010 LYCIV Zhoushan RSIV Ehime-1 LYCIV	100.00%	ORF 066R	99.44%	ORF 388R	100.00%	[1] 4L	91.78%	4L	97.89%
ORF 068R	70413	71196	486	hypothetical protein	RSIV subtype I	LYCIV Zhoushan	100.00%	ORF 067R	96.30%	ORF 390R	99.79%	3L	90.00%		86.59%
ORF 069R	71268	71735	468	DNA dependent RNA polymerase subunit H like protein	RSIV subtype I	PIV2016 PIV2014a PIV2010 LYCIV Zhoushan RSIV Ehime-1 LYCIV	100.00%	ORF 068R	99.36%	RPOH	100.00%	2R	93.83%	2R	94.25%
ORF 070R	71705	72841	1137	probable transmembrane amino acid transporter	RSIV subtype I	PIV2016 PIV2014a PIV2010 LYCIV Zhoushan RSIV Ehime-1 LYCIV	100.00%	ORF 069R	97.89%	ORF 396R	100.00%	1L	93.23%	1L	92.52%
ORF 071R	72956	73672	717	hypothetical protein	RSIV subtype II	RSIV RIE12-1 RSIV KagYT-96 GSIV-K1 OSGIV	100.00%	ORF 070R	99.86%	ORF 401R	98.61%	124L	93.01%	115L	92.39%
ORF 072R	73681	74061	381	hypothetical protein	RSIV subtype II	RSIV KagYT-96 RSIV RIE12-1 GSIV-K1 RBIV-C1 RSIV_121 OSGIV 17RbGs	100.00%	ORF 071R	100.00%	ORF 407R	98.69%	123R	97.58%	114R	95.90%
ORF 073L	74033	74752	720	ATPase(adenosine triphosphatase) [2]	RSIV subtype II	RSIV KagYT-96 RSIV RIE12-1 GSIV-K1 RBIV-C1 RSIV_121 OSGIV 17RbGs	100.00%	ORF 072L	100.00%	ORF 412L	99.03%	122R	95.97%	113R	95.97%
ORF 074R	74762	75397	636	hypothetical protein	RSIV subtype II	RSIV KagYT-96 RSIV RIE12-1 GSIV-K1 RBIV-C1 RSIV_121 OSGIV	97.48%	ORF 073R	97.48%	ORF 413R	97.16%	121L	86.09%	112L	84.54%
ORF 075L	75418	75924	507	hypothetical protein	RSIV subtype II	RSIV KagYT-96 GSIV-K1 RBIV-C1 RSIV_121 OSGIV 17RbGs	100.00%	ORF 074L	100.00%	ORF 420L	97.24%	120R	93.53%	111R	92.28%
ORF 076L	75955	76242	288	probable transcriptional activator RING-finger domain-containing E3 protein	RSIV subtype II	RSIV KagYT-96 RSIV RIE12-1 GSIV-K1 RBIV-C1	100.00%	ORF 075L	100.00%	ORF 423L	98.96%	119R	93.71%	110R	92.01%

						RSIV_121 OSGIV 17RbGs									
ORF 077R	76312	77625	1314	ankyrin repeat-containing protein	RSIV subtype II	RSIV KagYT-96 RSIV RIE12-1 GSIV-K1	100.00%	ORF 076R	99.77%	ORF 424R	96.88%	118L	93.03%	109L	92.03%
ORF 078R	77958	78632	675	FV3 early 31KDa protein homolog	RSIV subtype II	RSIV KagYT-96 GSIV-K1 RSIV_121 OSGIV	99.85%	ORF 077R	99.85%	ORF 436R	98.22%	117L	93.79%	108L	94.82%
ORF 079L	78686	80062	1377	hypothetical protein	RSIV subtype II	RSIV KagYT-96 RSIV RIE12-1 GSIV-K1 17RbGs	100.00%	ORF 078L	100.00%	ORF 450L	96.27%	116R	86.68%	107R	85.92%
ORF 080L	80123	81133	1011	immediate-early protein ICP46 [2]	RSIV subtype II	RSIV KagYT-96 RSIV RIE12-1 GSIV-K1 RBIV-C1 RSIV_121 17RbGs	100.00%	ORF 079L	100.00%	ORF 458L	98.32%	115R	93.18%	106R	93.08%
ORF 081R	81568	84150	2583	putative tyrosine kinase [2]	RSIV subtype II	GSIV-K1	100.00%	ORF 080R	99.96%	ORF 463R	97.99%	114L	93.69%	105L	93.26%
ORF 082L	84194	84574	381	hypothetical protein	RSIV subtype II	RSIV KagYT-96 RSIV RIE12-1 GSIV-K1 RBIV-C1 RSIV_121 OSGIV	100.00%	ORF 081L	99.74%	ORF 483L	97.38%	113R	92.66%	104R	92.89%
ORF 083L	84682	85425	744	proliferating cell nuclear antigen [2]	RSIV subtype II	RSIV KagYT-96 RSIV RIE12-1 GSIV-K1 RBIV-C1 RSIV_121 OSGIV 17RbGs	100.00%	ORF 082L	100.00%	ORF 487L	98.39%	112R	94.35%	102R	96.01%
ORF 084R	85445	86341	897	tumor necrosis factor recepter - assosiated factor-like protein	RSIV subtype II	RSIV KagYT-96RSIV RIE12-1GSIV-K1RBIV-C1RSIV_12117RbGs	100.00%	ORF 083R	100.00%	ORF 488R	97.99%	111L	93.09%	101L	90.41%
ORF 085L	86338	86493	156	hypothetical protein	RSIV subtype II	RSIV KagYT-96 RSIV RIE12-1 GSIV-K1 RBIV-C1 RSIV_121 RBIV-KOR-TY1 OSGIV 17RbGs	100.00%	ORF 084L	100.00%	ORF 492L	96.79%	[1] 110R	90.38%	100R	91.03%
ORF 086R	86546	89308	2763	D5 family NTPase [2]	RSIV subtype II	RSIV KagYT-96 RSIV RIE12-1 GSIV-K1 OSGIV	100.00%	ORF 085R	99.96%	ORF 493R	97.79%	109L	94.29%	99L	94.53%
ORF 087R	89389	90018	630	hypothetical protein	RSIV subtype II	RSIV RIE12-1 GSIV-K1 RBIV-C1 RSIV_121	99.84%	ORF 086R	99.84%	ORF 502R	95.67%	108.5L	91.61%	98L	94.91%

						RBIV-KOR-TY1 OSGIV									
ORF 088R	90058	90930	873	hypothetical protein	RSIV subtype II	RSIV KagYT-96 RSIV RIE12-1 GSIV-K1 RBIV-C1 OSGIV 17RbGs	100.00%	ORF 087R	100.00%	ORF 506R	97.25%	-	-	97L	80.25%
ORF 089L	90937	91901	888	HIT-like protein	RSIV subtype II	RSIV KagYT-96 RSIV RIE12-1 GSIV-K1 OSGIV	99.89%	ORF 088L	99.55%	ORF 515L	96.83%	-	-	-	-
ORF 090L	91953	92324	372	hypothetical protein	RSIV subtype II	RSIV KagYT-96 RSIV RIE12-1 GSIV-K1 RBIV-C1 RSIV_121 RBIV-KOR-TY1 OSGIV 17RbGs	100.00%	ORF 089L	100.00%	ORF 518L	98.66%	105R	95.99%	96R	94.62%
ORF 091L	92326	93102	777	hypothetical protein	RSIV subtype II	RSIV KagYT-96 RSIV RIE12-1 GSIV-K1 RBIV-C1 RSIV_121 OSGIV	98.71%	ORF 090L	98.71%	ORF 522L	98.20%	104R	94.21%	95R	90.09%
ORF 092L	93164	93577	414	suppressor of cytokine signalling 1 homolog	RSIV subtype I	PIV2016 PIV2014a PIV2010 LYCIV Zhoushan RSIV Ehime-1	100.00%	ORF 091L	95.17%	ORF 524L	100.00%	103R	88.38%	94R	88.22%
ORF 093L	93584	95029	1446	ankyrin repeat containing protein	RSIV subtype I	PIV2016 PIV2014a PIV2010 LYCIV Zhoushan RSIV Ehime-1	100.00%	ORF 092L	97.99%	ORF 534L	100.00%	102R	91.46%	93R	92.39%
ORF 094R	95098	95613	516	hypothetical protein	RSIV subtype I	PIV2016 PIV2014a PIV2010 LYCIV Zhoushan RSIV Ehime-1	100.00%	ORF 093R	97.29%	ORF 535R	100.00%	101L	93.80%	92L	92.83%
ORF 095R	95588	96229	642	hypothetical protein	RSIV subtype II	RSIV KagYT-96 RSIV RIE12-1 GSIV-K1 OSGIV	99.07%	ORF 094R	98.75%	ORF 539R	98.91%	100L	86.49%	91L	86.67%
ORF 096R	96283	96606	324	RING-finger-containing E3 ubiquitin ligase	RSIV subtype II	RSIV KagYT-96 GSIV-K1 RBIV-C1 RSIV_121 RBIV-KOR-TY1 OSGIV 17RbGs	100.00%	ORF 095R	100.00%	ORF 543R	97.53%	99L	91.05%	90L	84.26%
ORF 097R	96655	97146	492	hypothetical protein	RSIV subtype II	RSIV KagYT-96 RSIV RIE12-1	100.00%	ORF 096R	100.00%	ORF 545R	97.36%	97.5L	94.51%	89L	92.48%

						GSIV-K1 RBIV-C1 RSIV_121 OSGIV 17RbGs									
ORF 098R	97137	97888	738	hypothetical protein [2]	RSIV subtype II	RSIV KagYT-96 RSIV RIE12-1 GSIV-K1 RBIV-C1 RSIV_121 OSGIV 17RbGs	100.00%	ORF 097R	100.00%	ORF 550R	98.10%	96L	94.58%	88L	93.77%
ORF 099R	97896	99059	1164	hypothetical protein	RSIV subtype II	RSIV KagYT-96 RSIV RIE12-1 GSIV-K1 OSGIV	100.00%	ORF 098R	99.91%	ORF 554R	96.91%	95L	91.21%	87L	91.02%
ORF 100R	99084	99584	501	hypothetical protein	RSIV subtype II	RSIV KagYT-96 RSIV RIE12-1 GSIV-K1 RBIV-C1 RSIV_121 OSGIV 17RbGs	100.00%	ORF 099R	100.00%	ORF 562R	98.60%	94L	95.41%	86L	93.01%
ORF 101R	99594	100520	927	probable RNA binding protein	RSIV subtype II	RSIV KagYT-96RSIV RIE12-1GSIV-K1SKIVRBIV-C1RSIV_121OSGIV17RbGs	100.00%	ORF 100R	100.00%	ORF 569R	97.84%	93L	92.22%	85L	92.02%
ORF 102R	100641	101711	1071	myristoylated membrane protein [2]	RSIV subtype II	RSIV KagYT-96 RSIV RIE12-1 GSIV-K1 OSGIV	98.62%	ORF 101R	99.69%	ORF 575R	95.94%	-	-	83L	91.36%
ORF 103L	101692	103263	1572	hypothetical protein	RSIV subtype I	PIV2016 PIV2014a PIV2010 LYCIV Zhoushan	98.85%	ORF 102L	98.54%	ORF 586L	98.20%	88R	92.24%	82R	93.26%
ORF 104R	103311	103724	414	hypothetical protein	RSIV subtype II	RSIV KagYT-96 RSIV RIE12-1 GSIV-K1 RBIV-C1 RSIV_121 OSGIV	99.52%	ORF 103R	99.52%	ORF 591R	99.28%		94.31%	81R	95.48%
ORF 105L	103721	104518	798	RNase III-like ribonuclease [2]	RSIV subtype II	RSIV KagYT-96 RSIV RIE12-1 RBIV-C1 RSIV_121 17RbGs	100.00%	ORF 104L	100.00%	RNC	97.99%	87R	94.16%	80R	94.86%
ORF 106L	104484	104951	468	Uvr/REP helicase [2]	RSIV subtype II	RSIV KagYT-96 RSIV RIE12-1 GSIV-K1 OSGIV	100.00%	ORF 105L	93.80%	ORF 600L	97.44%	86R	92.55%	79R	92.95%
ORF 107L	104948	105451	504	hypothetical protein	RSIV subtype II	RSIV KagYT-96 RSIV RIE12-1 GSIV-K1	100.00%	ORF 106L	92.86%	ORF 605L	97.83%	85R	92.74%	78R	90.73%

						RBIV-C1 RSIV_121 RBIV-KOR-TY1 OSGIV									
ORF 108R	105565	106869	1305	hypothetical protein	RSIV subtype II	RSIV KagYT-96 RSIV RIE12-1 GSIV-K1 OSGIV	100.00%	ORF 107R	95.21%	ORF 606R	97.70%	84L	93.16%	77L	91.58%
ORF 109L	106896	107255	360	hypothetical protein	RSIV subtype II	RSIV KagYT-96 RSIV RIE12-1 GSIV-K1 RBIV-C1 RSIV_121 OSGIV	100.00%	ORF 108L	98.89%	ORF 617L	98.33%	83R	93.46%	76R	92.48%
ORF 110R	107319	108425	1107	hypothetical protein	RSIV subtype II	RSIV KagYT-96 RSIV RIE12-1 GSIV-K1 OSGIV	100.00%	ORF 109R	99.82%	ORF 618R	97.92%	82L	93.59%	75L	93.22%
ORF 111L	108474	108971	498	hypothetical protein	RSIV subtype II	RSIV KagYT-96 RSIV RIE12-1 GSIV-K1 RBIV-C1 RSIV_121 OSGIV 17RbGs	100.00%	ORF 110L	100.00%	ORF 628L	97.99%	81R	95.78%	74R	94.32%
ORF 112L	108984	109457	474	hypothetical protein	RSIV subtype II	RSIV KagYT-96 RSIV RIE12-1 GSIV-K1 RBIV-C1 RBIV-KOR-TY1 OSGIV 17RbGs	100.00%	ORF 111L	100.00%	ORF 632L	95.81%	-	-	73R	85.56%
ORF 113R	109545	109769	225	hypothetical protein	RSIV subtype II	RSIV KagYT-96 RSIV RIE12-1 GSIV-K1 RBIV-C1 RSIV_121 OSGIV 17RbGs	100.00%	ORF 112L	100.00%	ORF 634L	92.06%	79L	93.78%	72L	92.27%
ORF 114L	109771	110235	465	hypothetical protein	RSIV subtype II	RSIV KagYT-96 RSIV RIE12-1 GSIV-K1 RBIV-C1 RSIV_121 OSGIV 17RbGs	100.00%	ORF 113L	100.00%	ORF 635L	97.42%	78R	96.34%	71R	93.76%
ORF 115L	110232	111566	1335	hypothetical protein	RSIV subtype II	RSIV KagYT-96 RSIV RIE12-1 GSIV-K1 RBIV-C1 OSGIV	99.93%	ORF 114L	99.93%	ORF 641L	96.55%	77R	90.95%	70R	90.42%

Table 5. ORF locations of the 26 conserved core genes conserved in the family Iridoviridae

No.	Gene (GenBank access. No.)	17SbTy (OK042108)	17RbGs (OK042109)	Ehime-1 (AB104413)	ISKNV (AF371960)	RBIV (AY532606)	TRBIV (GQ273492)
1	hypothetical protein	001R	001R	639R	76L	72L	69L
2	Putative NTPase I	013R	012R	NTPase	63L	59L	58L
3	Putative replication factor and/or DNA binding-packing	015R	014R	092R	61L	57L	56L
4	Helicase family	018R	017R	101R	56L	54L	53L
5	Serine-threonine protein kinase	019R	018R	106R	55L	53L	52L
6	Erv1/Alr family	031R	030R	156R	43L	43.5L	42L
7	DNA dependent RNA polymerase second largest subunit	040L	039L	RPO-2	34R	33R	33R
8	Deoxynucleoside kinase	042L	041L	TK	32R	31R	31R
9	Transcription elongation factor TFIIS	044R	043R	238R	29L	29.5Lb	29L
10	DNA dependent RNA polymerase largest subunit	045R	044R	RPO-1	28L	29L	26L
11	Putative XPPG-RAD2-type nuclease	046R	045R	256R	27L	28L	27L
12	Ribonucleotide reductase small subunit	048L	047L	RR-2	24R	26R	25R
13	DNA pol Family B exonuclease	052L	051L	DPO	19R	20R	20R
14	Serine-threonine protein kinase	058L	057L	349L	13R	13R	13R
15	Myristoylated membrane protein	064R	063R	374R	7L	8L	7L
16	Major capsid protein	065R	064R	MCP	6L	7L	6L
17	NIF-NLI interacting factor	066R	065R	385R	5L	6L	5L
18	ATPase(adenosine triphosphatase)	073L	072L	412L	122R	116R	113R
19	Immediate early protein ICP-46	080L	079L	458L	115R	108.5R	106R
20	Putative tyrosin kinase/lipopolysaccharide modifying enzyme	081R	080R	463R	61L, 114L	57L, 106Lb	105L
21	Proliferating cell nuclear antigen	083L	082L	487L	112R	103Rb	102R
22	D5 family NTPase involved in DNA replication	086R	085R	493R	109L	101L	99L
23	hypothetical protein	098R	097R	550R	96L	89.5Lb	88L
24	Myristoylated membrane protein	102R	101R	575R	90.5L	85L	83R
25	RNase III-like ribonuclease	105L	104L	RNC	87R	83R	80R
26	Uvr/REP helicase	106L	105L	600L	86R	82.5R	79R

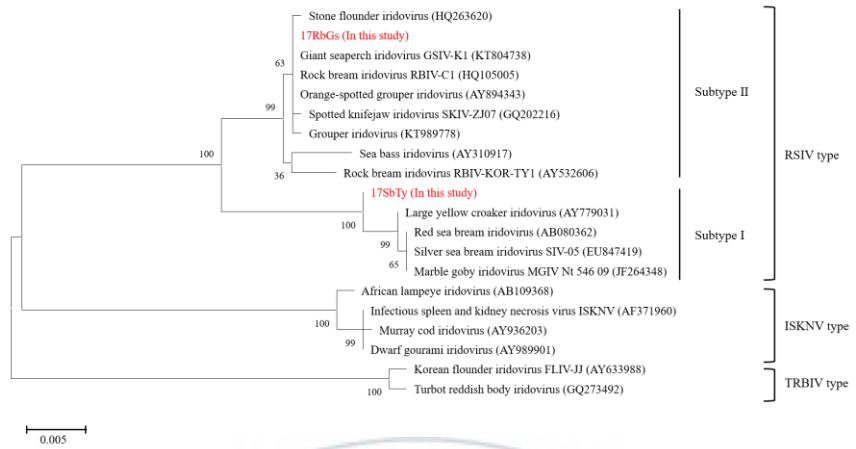

(A)

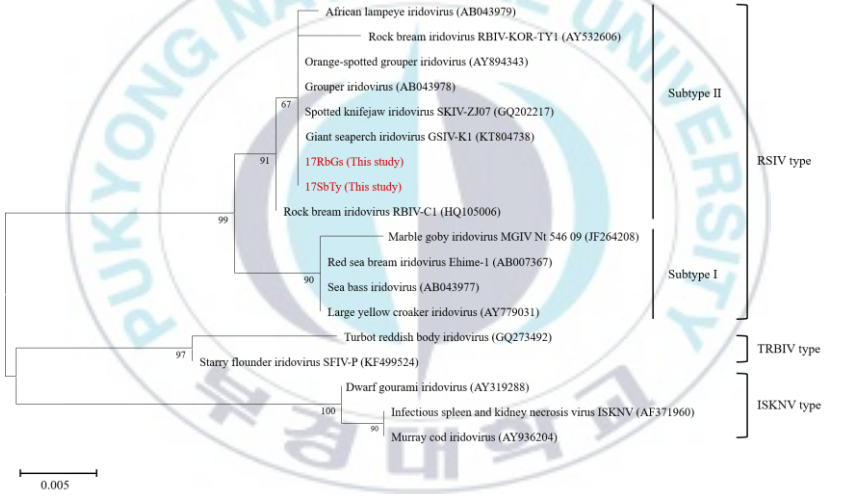

(B)

Figure 2. Phylogenetic trees based on the complete nucleotide sequences of the (A) major capsid protein gene (MCP; 1,362 bp) and (B) adenosine triphosphatase gene (ATPase; 721 bp) of two red sea bream iridovirus (RSIV) isolates (17SbTy and 17RbGs) collected from cultured fish in Korea. The phylogenetic trees were constructed using the maximum-likelihood method in MEGA (ver. 11). Bootstrap values were obtained from 1,000 replicates, and the scale bar represents 0.005 nucleotide substitutions per site. The two RSIV isolates (17SbTy and 17RbGs) from this study are highlighted in bold and red color.

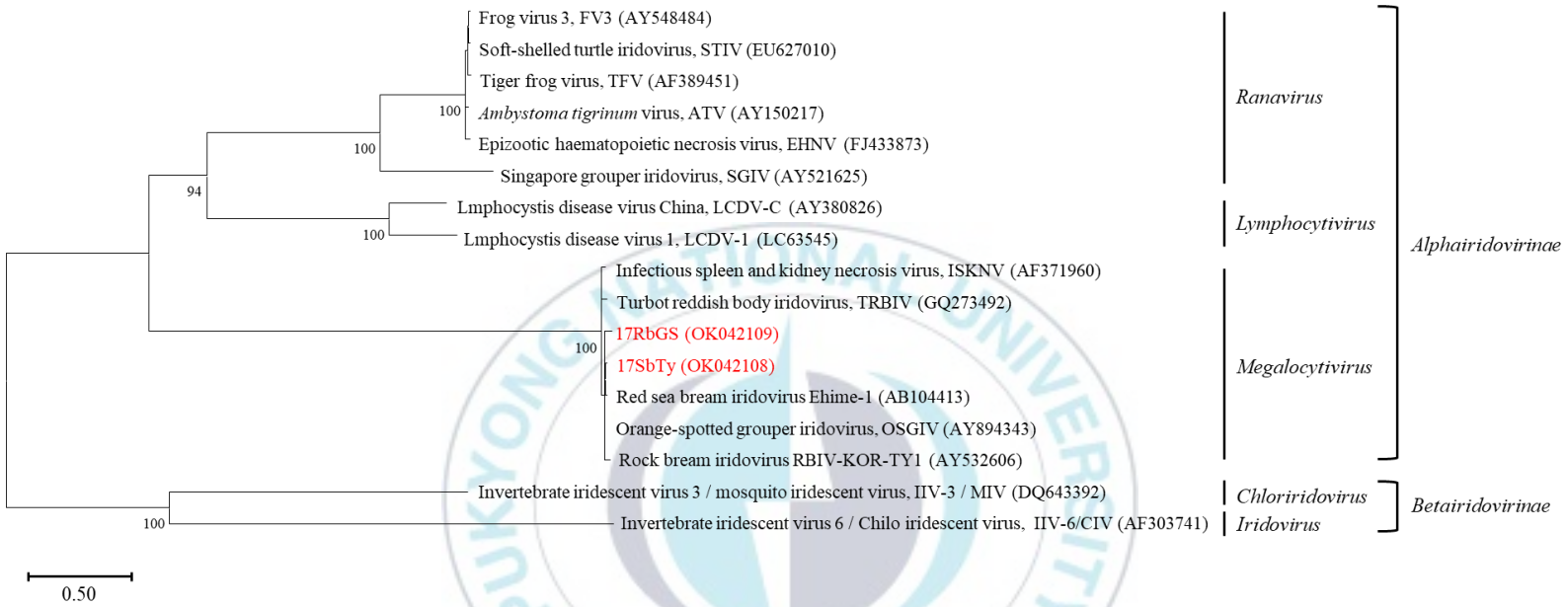

Figure 3. Phylogenetic trees based on the deduced amino acid sequences of the 26 concatenated genes conserved among all members of the family *Iridoviridae*. The tree was constructed via the maximum-likelihood method under LG model and gamma-distributed with invariant sites (LG + G4 + I) in MEGA (ver. 11). The two RSIV isolates (17SbTy and 17RbGs) from this study are highlighted in bold and red color.

1-3. Insertions/deletions

The complete genome of 17SbTy showed 133 InDels when compared to Ehime-1 and 17RbGs (data not shown). Notably, the positions 10,693-14,853 in the 17SbTy (4161 bp) encodes two functional proteins–an mRNA-capping enzyme (ORF 012R, positions 10,693–12,165 in the 17SbTy genome) and a putative NTPase I (ORF 013R, positions 12,205–14,853 in the 17SbTy genome). However, the positions 10690-14844 in the 17RbGs genome (4155 bp) of 99.78% homology with 17SbTy possesses only a single functional protein (ORF 012R). This region of 17RbGs identified a 6 bp deletion, including a stop codon (TGA) and an intergenic codon (CCT) compared 17SbTy (ORF 012R and 013R), Ehime-1 (MCE and NTPase), and RBIV-KOR-TY 1 (ORF 060L and 069L) and this deletion caused a frameshift mutation (Figure 4).

Among the InDel regions in 17SbTy identified when it was compared to Ehime-1 and 17RbGs, 18 regions contain >10 bp mutations, and only four InDels were identified in coding regions (ORFs 014R, 053R, 054R, and 102R in 17SbTy). Of the InDels found in the ORFs known to encode functional proteins, a 30 bp deletion in myristoylated membrane protein was identified in ORF 101R of 17RbGs compared 17SbTy (ORF 102R), Ehime-1 (ORF 575R), and RBIV-KOR-TY 1 (ORF 86L; Figure 5D). Furthermore, a 27 bp deletion in a DNA-binding protein was identified in 17SbTy (ORF 014R), in 17RbGs (ORF 013R), and RBIV-KOR-TY 1 (ORF 058L), but not in the Ehime-1 (ORF 077R; Figure 5A). Two other ORFs (ORF 053R and 054R in 17SbTy) have not yet been functionally characterized (Figure 5B and C) and a 19 bp deletion was identified in ORF 052R of 17RbGs compared

17SbTy (ORF 053R), Ehime-1 (ORF 318R), and RBIV-KOR-TY 1 (ORF 018,019L; Figure 5B). On the other hand, a 27 bp insertion was identified in 17RbGs (ORF 053R) and RBIV-KOR-TY 1 (ORF 17L), but not in the 17SbTy (ORF 054R) and Ehime-1 (ORF 077R; Figure 5C).

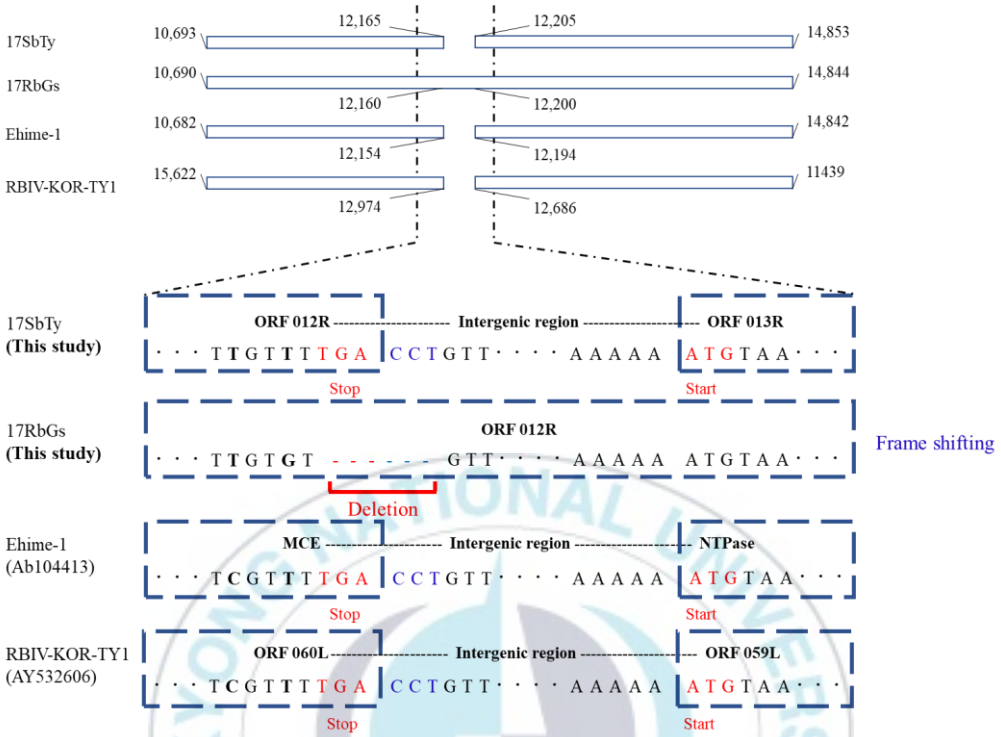

Figure 4. Schematic representation of a deletion of the termination codon in ORF 012R of 17RbGs causing a frameshift mutation. The aligned sequences are genomes of 17SbTy, 17RbGs, and two representative RSIVs (Ehime-1 [RSIV subtype I] and RBIV-KOR-TY1 [RSIV subtype II]). The boxes consisting of blue dashed lines represent the coding regions. The termination and start codons are shown in red, and the deleted sequences in the intergenic region are highlighted in blue.

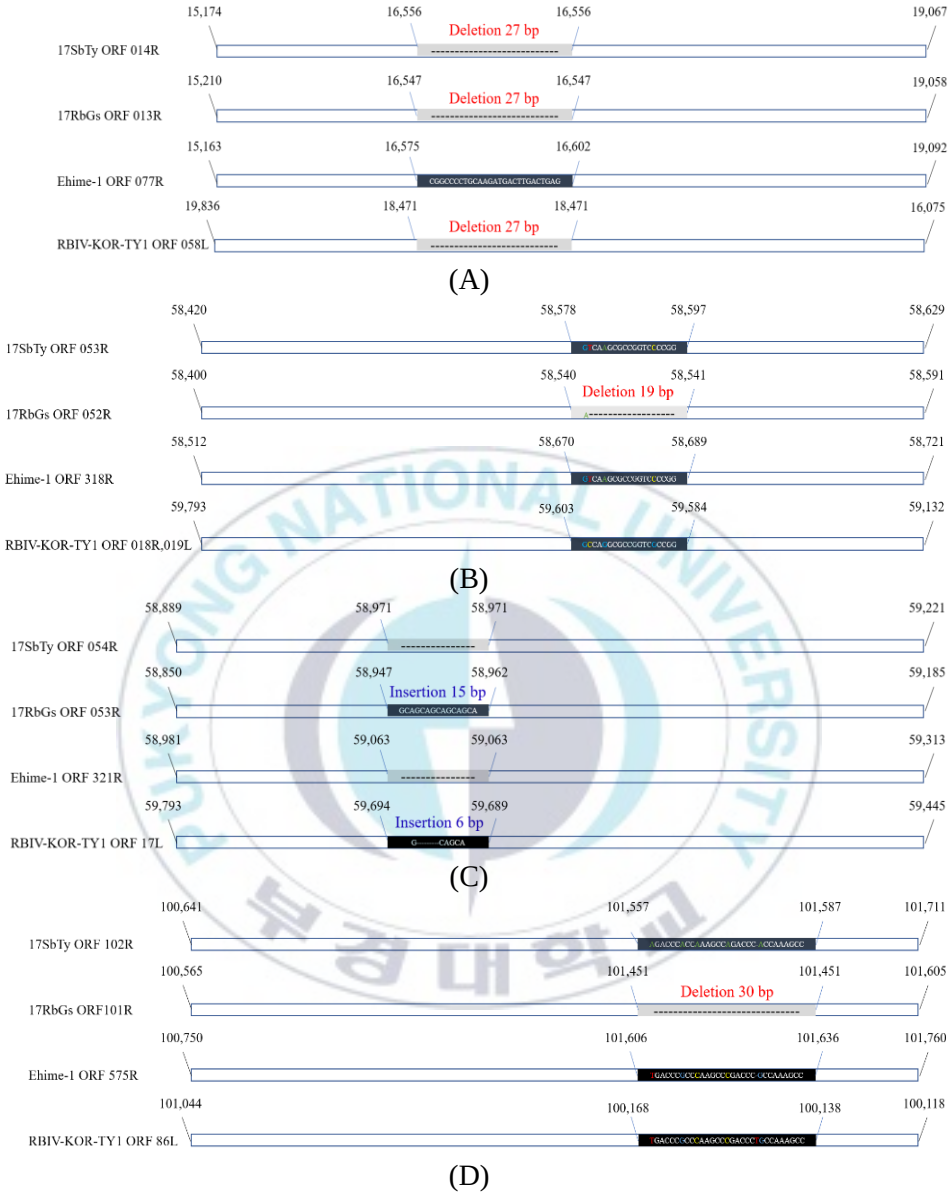

Figure 5. Schematic representation of insertion/deletion mutations (InDels) (>10 bp) in the coding regions of 17SbTy when compared with those of 17RbGs and two representatives RSIVs (Ehime-1 [RSIV subtype I] and RBIV-KOR-TY1 [RSIV subtype II]). The numbers indicate the positions of the InDels in the genome; white bars represent genome fragments, black bars denote insertions, and gray bars represent deletions.

2. Virulence evaluation of the RSIV isolates

2-1. Viral replication in RBF cell (*in vitro*)

The viral genome copy number of extracellular RSIV released from the infected RBF cells is shown in Figure 6. At 1 dpi., viral genome copy numbers of 17RbGs were slightly reduced by PBS washing to eliminate un-binding or non-penetrating viral particles after 1 h of absorption. Viral genome copies of both extracellular RSIVs released from infected RBF cells increased at 3, 5, 7, and 9 dpi, with significant differences between 17SbTy and 17RbGs ($P < 0.05$). The maximum amounts of 17SbTy and 17RbGs in the culture medium of RBF cells were approximately 10-fold different, 4.09×10^7 at 9 dpi and 3.94×10^8 viral genome copies/mL at 11 dpi, respectively.

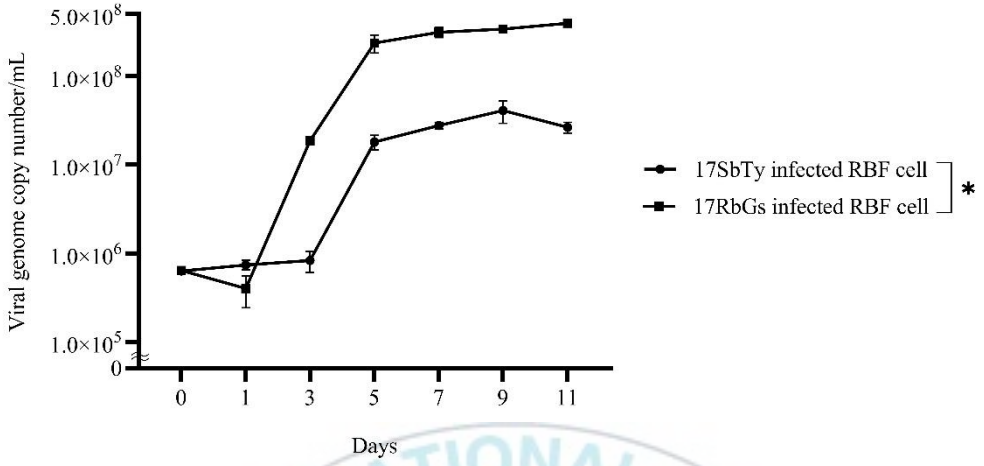

Figure 6. Comparison of the viral genome copy numbers (means ± SD) for extracellular red sea bream iridovirus (RSIV) after two RSIVs (17SbTy and 17RbGs isolates) inoculation to rock bream fin cell. A significant difference in the numbers of viral genome copies between RSIV isolates was supported by two-way ANOVA analysis (*, $P < 0.05$).

2-2. Pathogenicity of two RSIVs against rock bream (*in vivo*)

2-2-1. Pathogenicity of two RSIVs against rock bream

In challenge tests, the survival rates of each RSIV-injected rock bream (1×10^4 viral genome copies/fish of 17RbGs and 17SbTy) and native rock bream (control group) were evaluated. The mortality to 17RbGs infected group was annihilation within seven days from the first emergence of dead fish (7 dpi). 17SbTy infected group also died during a week from 10 dpi and 28.6% (6/21) of the infected rock bream survived 21 days post-injection (Figure 7). The difference in the survival rates between the 17SbTy- and 17RbGs-infected rock breams was significant (log-rank test, $P < 0.05$). The nucleotide sequences of the four InDel regions (ORFs 014R, 053R, 054R and 102R on the basis of the 17SbTy isolate) completely matched between the cell-cultured isolates and viruses from dead fish (data was not shown).

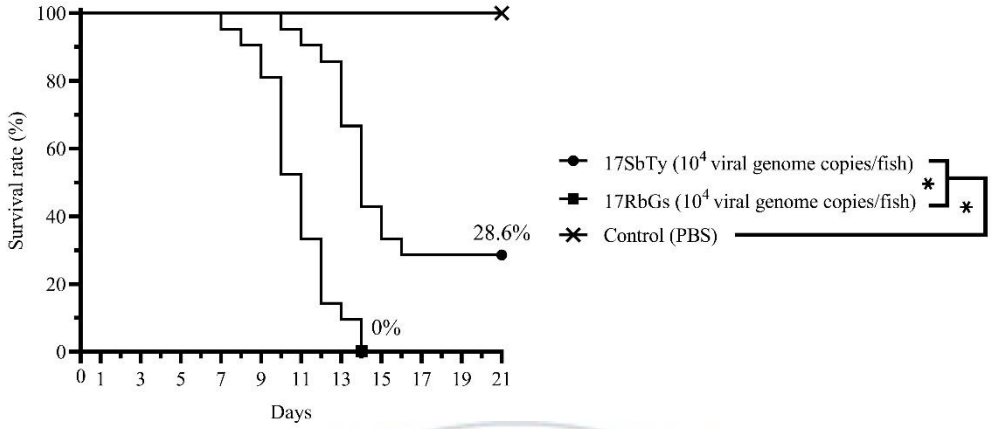

Figure 7. Survival rates (%) of rock breams after intraperitoneal injection with the two RSIV isolates (either 17SbTy or 17RbGs, 10^4 genome copies per fish). Statistical analysis was performed by the log-rank test (*$P < 0.05$).

2-2-2. Odds ratio

Based on the spleen index and two major clinical signs of RSIVD (abnormal swimming and lethargy), the odds ratio of rock bream after IP injection with RSIV isolates was significantly different compared with the control group (Table 6). Among a total of 21 experimental fish, the numbers of infected or uninfected cases with clinical signs for rock bream after IP injection with 17SbTy isolate were 9 and 12, respectively, different from the findings in the 17RbGs injected rock bream (16 and 5, respectively). The infected case with clinical signs of rock bream injected with 17SbTy isolate showed 55.6% (5/9) spleen index overvalue (> 3), 88.9% (8/9) abnormal swimming, and 22.2% (2/9) lethargy. Meanwhile, rock bream injected with 17RbGs isolate revealed 68.8% (11/16), 93.8% (15/16), and 68.8% (11/16) of infected cases with clinical signs, different from rock bream after 17SbTy infection. In addition, rock bream injected with 17SbTy and 17RbGs isolates showed 16.7% (2/12) and 20.0% (1/5) spleen index overvalue, respectively, consistent with the uninfected case with clinical signs. In both RSIV-injected rock bream groups, no abnormal swimming or lethargy was observed in the uninfected cases with clinical signs. The odds ratios based on the spleen index overvalue, abnormal swimming and lethargy for 17SbTy infection represented 19.38, 9.00 and 1.29, different from finding in 17RbGs infection were they more highly evaluated as 55.00, 16.00, and 3.20 in those ratios, respectively (Table 6).

Table 6. Odds ratio based on the probability of infection with clinical signs after infection with each RSIV isolate compared to control group

Symptomatology	Total (*n*=21)	17SbTy		Control	Odds ratio	95 % confidence interval		*P*-value
		infected case with clinical sign	uninfected case with clinical sign	with clinical sign		upper	down	
Spleen index (> 3)[a]	16.7 % (7/42)	55.6 % (5/9)	16.7 % (2/12)	0 % (0/21)	19.38	2.78	135.16	*[b]
Abnormal swimming	19.0 % (8/42)	88.9 % (8/9)	0.0 % (0/12)	0 % (0/21)	9.00	1.42	57.12	*
Lethargy	4.8 % (2/42)	22.2 % (2/9)	0.0 % (0/12)	0 % (0/21)	1.29	0.91	1.82	ns[c]
Symptomatology	**Total (*n*=21)**	**17RbGs**		**Control**	**Odds ratio**	**95 % confidence interval**		***P*-value**
		infected case with clinical sign	uninfected case with clinical sign	with clinical sign		upper	down	
Spleen index (> 3)[a]	38.1 % (16/42)	68.8 % (11/16)	20.0 % (1/5)	0 % (0/21)	55.00	5.73	527.66	*
Abnormal swimming	54.8 % (23/42)	93.8 % (15/16)	0.0 % (0/5)	0 % (0/21)	16.00	2.40	106.73	*
Lethargy	26.2 % (11/42)	68.8 % (11/16)	0.0 % (0/5)	0 % (0/21)	3.20	1.55	6.62	*

[a] over value for mean spleen index in RSIV injected fish as > 3;
[b] *P*-value was supported by chi-squared test using SPSS program ($P < 0.05$);
[c] ns, not significant difference

2-2-3. RSIV shedding ratio

To compare the viral shedding rate (virus released from RSIV-infected rock bream) and the number of viral genome copies in the spleen (virus within the host), the viral genome copy numbers of spleen tissue and rearing water were quantified by interval times (1, 3, 5, 7, 9, 11, and 14 days post-IP injection). The maximum numbers of viral genome copies in the spleen after IP injection with 17SbTy and 17RbGs were 6.48×10^7 and 3.00×10^{10} viral genome copies/g tissue at 11 days, respectively (Figure 8). The maximum viral shedding rate showed 1.23×10^5 and 7.76×10^5 viral genome copies number/L/g at 14 days after IP injection with 17SbTy and 17RbGs (Figure 8). Notably, a significant difference in the viral shedding ratio and the number of viral genome copies in the spleen between 17SbTy- and 17RbGs-infected rock bream was identified at 11 and 14 days post-infection ($P < 0.05$).

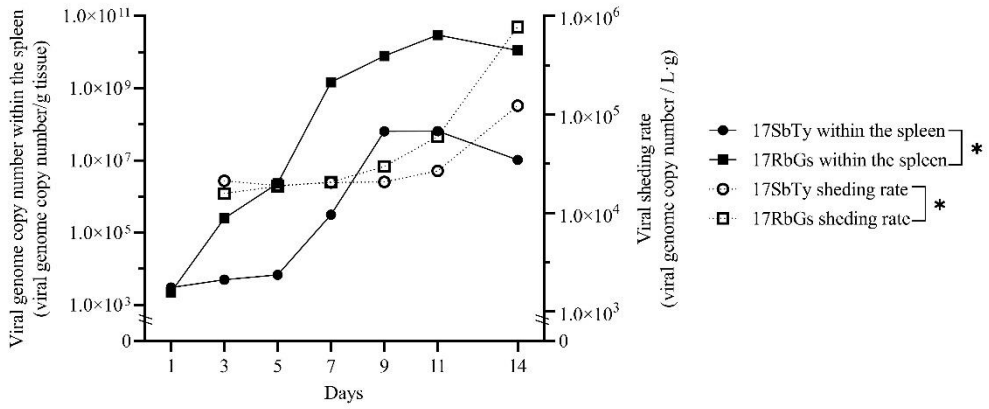

Figure 8. Viral shedding ratio and viral genome copy number of the spleen after infection with two red sea bream iridovirus (RSIV) isolates. Based on the number of viral genome copies in rearing water and spleen, viral shedding ratio (viral genome copy number/L/g) was determined. A significant difference was supported by two-way ANOVA analysis (*, $P < 0.05$).

2-3. Evaluation of mortality using cohabitation challenge

Under natural mimic conditions, the mortalities of native rock bream (recipient group) cohabitated with two doses (1×10^4 viral genome copies/fish as the high dose; 1×10^2 viral genome copies/fish as the low dose) of each RSIV-injected rock bream (donor group) were evaluated. In the high-dose challenge test, rock bream showed 100% cumulative mortality within 12 days of IP injection with 17RbGs, which significantly differed from that with 17SbTy-infected rock bream (53.33 %) for 21 days (Figure 9A). In addition, recipient rock bream cohabitated with 17RbGs and 17SbTy-injected rock bream exhibited significantly different mortality rates of 86.67% and 46.67%, respectively. In low-dose conditions, the cumulative mortality of each donor and recipient rock bream between RSIV isolates also showed significant differences, similar to the high-dose conditions. Even though 17RbGs-donor and recipient rock bream showed 80% cumulative mortality, the time for the initial emergence of dead fish was different (10 days after injection in the donor group and 13 days after cohabitation in the recipient group) (Figure 9B). In the 17SbTy group, donor rock bream showed 33.33% cumulative mortality within 18 days after IP injection, which was significantly different from the finding in the recipient rock bream showing 6.67% cumulative mortality for 21 days.

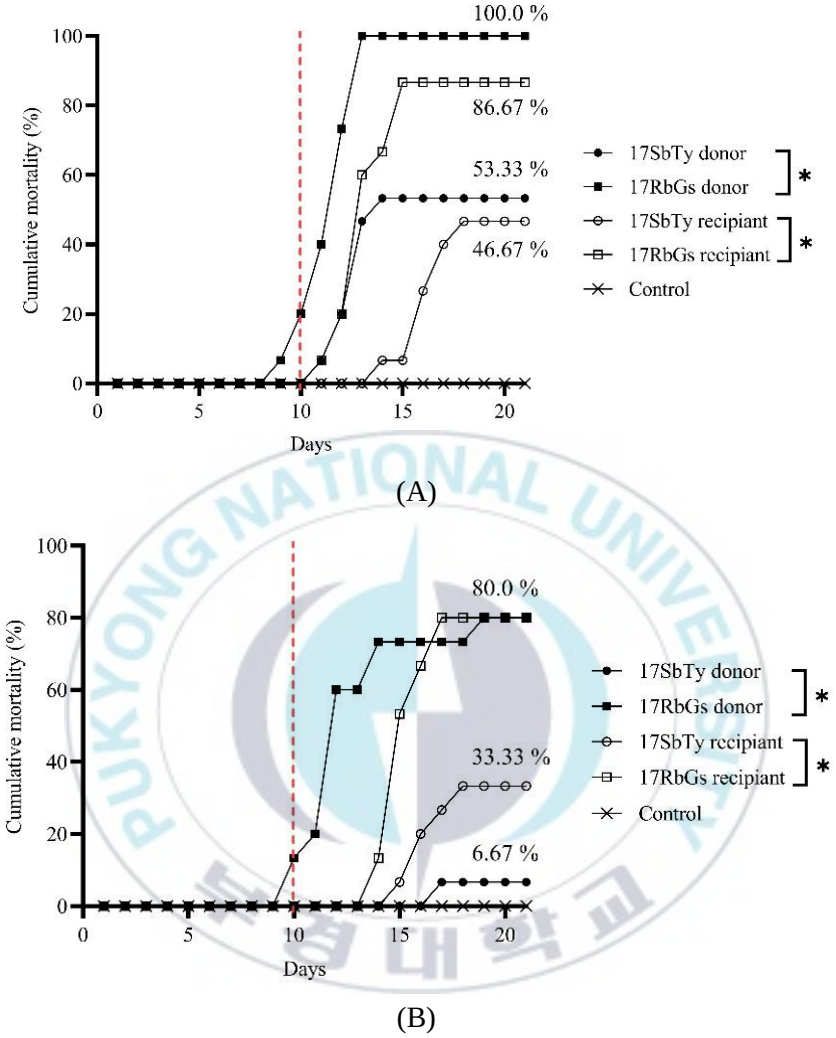

Figure 9. Cumulative mortality (%) of rock bream after two red sea bream iridovirus (RSIV) infections with different doses according to cohabitation challenge. (A) cohabitated with rock bream (donor) injected with high dose (10^4 viral genome copies/fish) and naïve fish (recipient); (B) cohabitated with rock bream (donor) injected with low dose (10^2 viral genome copies/fish) and naïve fish (recipient). RSIV-infected fish (donor) showed first death at 10 days after injection (dot line). RSIV exposed rock bream (recipient fish) by cohabitation were observed for 21 days. Statistical data were obtained using the log-rank test (*, $P < 0.05$).

2-4. Expression of viral and apoptosis-related genes

Based on the genetic difference in a DNA-binding protein and myristoylated membrane protein between 17SbTy and 17RbGs isolates, the expression of viral genes and apoptosis-related genes (caspase-3, -8 and PDCD 10) in rock bream after IP injection with RSIVs was evaluated. All viral genes were significantly upregulated at 2 and 3 days after RSIV injection (Figure 10A). Polymerase and major capsid protein genes, known to be essential for viral replication, were upregulated in the spleen of both 17SbTy-and 17RbGs-infected rock bream, and a 1.2-fold significant increase was found in the 17RbGs than in the 17SbTy group at 11 days post-infection (Figure 10A). The upregulated expression of genes encoding a DNA binding protein and myristoylated membrane protein of 17RbGs was identified as a 1.7-fold increase in both genes compared to the 17SbTy group at 11 days post-infection. Furthermore, even though the PDCD 10 gene was upregulated in both RSIV isolates without a significant difference, the expression levels of caspase-3 and -8 genes in the spleen derived from 17RbGs-infected rock bream were 1.2-and 2.95-fold higher than that in the 17SbTy group at 11 days post-infection (Figure 10B). Moreover, rock bream injected with two RSIV isolates showed a statistically significant differential expression in all viral genes and caspase-8 genes ($P < 0.05$), and these genes expressed early and were more upregulated in the 17RbGs-infected fish.

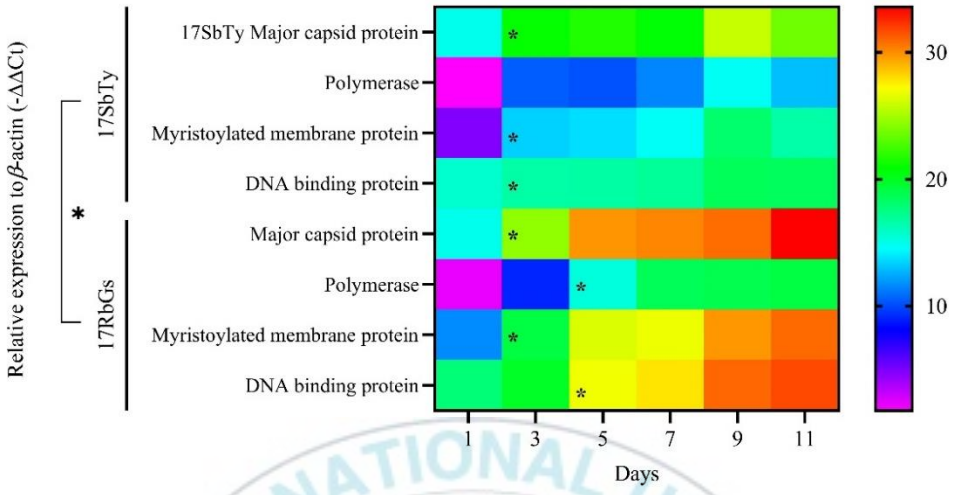

(A)

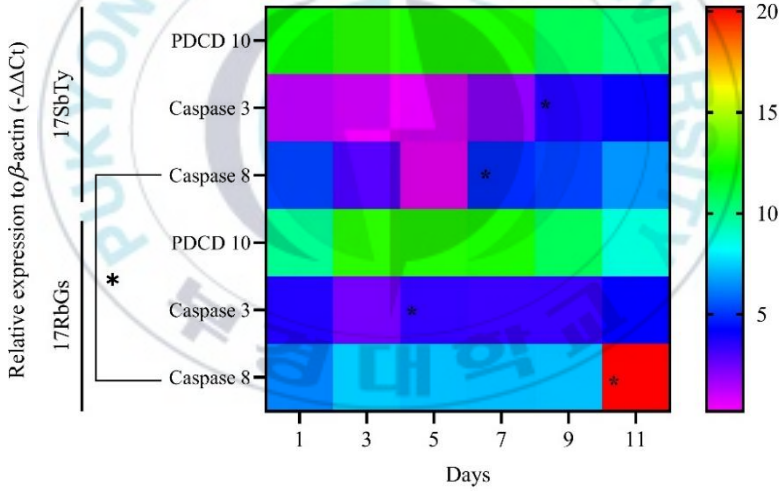

(B)

Figure 10. Heat map analysis of (A) viral genes (major capsid protein, polymerase, myristoylated membrane protein, DNA binding protein) and (B) apoptosis-related genes (PDCD10, caspase-3, and caspase-8) in the spleen of rock bream after two red sea bream iridovirus (RSIV) infections. Rainbow-colored bar denotes gene expression levels (-ΔΔCt value) compared with the control group. A significant difference was supported by two-way ANOVA analysis (*, $P < 0.05$).

IV. Discussion

Since the 1990s, RSIVD has been one of the problematic infectious diseases in marine and freshwater fish (OIE, 2021). Notably, the genetic variant including recombinant was emerged in RSIVD-endemic regions (Shiu *et al.*, 2018; Kim *et al.*, 2019). In this study, the different genotypes of RSIV, which belonged to either subtype I or II was identified from cultured Japanese seabass in Korea. To determine the genetic and pathogenicity characterization of that RSIV mixed subtype I/II (17SbTy isolate), the complete genome sequences and virulence were compared with RSIV subtype II (17RbGs), which is the predominant genotype in Korea.

The complete genomes of 17SbTy (122,360 bp), and 17RbGs (122,235 bp) turned out to be similar in size to most representative megalocytiviruses: RSIV (Ehime-1; 112,415 bp), ISKNV (112,080 bp), and TRBIV (110,104 bp), except for scale drop disease virus (GF_MU1; GenBank accession No. MT521409; 131,276 bp). The sequences were permuted and assembled into a circular form, similar to the format used for most megalocytiviruses (Figure 1). The 17RbGs belongs to RSIV subtype II, which has been the predominant genotype in marine fish in Korea since the 1990s (Kim *et al.*, 2019), based on the phylogeny of genes of MCP and ATPase. Of note, 17SbTy is grouped with either subtype I or II of RSIV depending on gene, respectively (Figure 2). A comparison of 17SbTy with Ehime-1 (ancestral RSIV subtype I) and 17RbGs (RSIV subtype II), showed 99.63% and 98.24% identity to the MCP gene and 99.03% and 100%

identity to the ATPase gene, respectively. Golden mandarin fish iridovirus, an RSIV subtype I reported in Korea in 2016 (Kim *et al.*, 2018), shares 99.9% sequence homology with Ehime-1 in both the MCP and ATPase genes. Unlike golden mandarin fish iridovirus, 17SbTy was classified as a mixed RSIV subtype (subtype I/II). The 17SbTy and 17RbGs are affiliated with the genus *Megalocytivirus* based on the phylogeny of the concatenated amino acid sequences of the 26 conserved genes (Figure 3; Table 5), which were known to be shared within *Iridoviridae* (Eaton *et al.*, 2007; Eaton *et al.*, 2010). The COG database was classified into four major groups involving a total of 26 functional categories (Galperin *et al.*, 2015). The annotated 20 protein-coding genes in both 17SbTy and 17RbGs in the COG database were assigned to only nine functional categories (Table 3; Figure 1): i) amino acid transport and metabolism; ii) nucleotide transport and metabolism; iii) translation, ribosomal structure, and biogenesis; iv) transcription; v) replication, recombination, and repair; vi) signal transduction mechanisms; vii) mobilome, prophages, transposons; viii) general function prediction only; and ix) function unknown. The nine functional categories identified in both 17SbTy and 17RbGs belong to all four major categories: metabolism, information storage and processing, cellular processes, and poorly characterized (Table 3).

Interestingly, 115 and 114 putative ORFs in 17SbTy and 17RbGs were predicted through NCBI annotation, respectively (Table 4). The complete nucleotide sequences of 17SbTy and 17RbGs turned out to be closely related to rock bream iridovirus-C1 (RBIV-C1, GenBank accession No. KC244182) belonging RSIV subtype II. Every 115

ORFs of 17SbTy which could be assigned functional proteins were best-matched to not only RSIV subtype II viruses (69 ORFs of 17SbTy) but also RSIV subtype I viruses (46 ORFs of 17SbTy) in detail (Table 4). In a previous study (Eaton *et al.*, 2007), several genes that code for different annotated ORFs within the family *Iridoviridae* contained frameshift mutations. Moreover, InDels are one of the causes of frameshift mutations that can affect the translation of a functional protein (Zhang *et al.*, 2013). A frameshift mutation caused by a short InDel [a 6 bp deletion, including a stop codon (TGA) and an intergenic codon (CCT)] proved to be the cause of the difference in the total number of ORFs between 17RbGs (n = 114) and 17SbTy (n = 115; Figure 4 and Table 4).

Notably, among the InDel regions between 17SbTy, 17RbGs, and Ehime-1, 18 regions are over 10bp in size and only four are distributed in coding regions (ORFs 014R, 053R, 054R, and 102R in 17SbTy). Although two ORFs code for known functional proteins (ORF 014R, which is involved in DNA binding, and ORF 102R, which is a myristoylated membrane protein; Figure 5A and D), two other ORFs (ORF 053R and 054R) have not yet been functionally characterized (Figure 5B and C). Of these two major InDels found in the ORFs known to encode functional proteins, a 27 bp deletion in a DNA-binding protein that has an FtsK-like domain was identified in 17SbTy (ORF 014R), in 17RbGs (ORF 013R), and RBIV-KOR-TY 1 (ORF 058L), but not in the Ehime-1 (ORF 077R; Figure 5A). The FtsK-like domain in the spotted knifejaw iridovirus (an RSIV-type) (Xiang *et al.*, 2014) participates in host immune evasion by inhibiting transcriptional activities of NF-κB and INF-γ, indicating that the deleted sequences that coded for the DNA-binding protein might affect viral replication

and/or pathogenicity in the host. Furthermore, ORF 102R of 17SbTy (Figure 5D), which is in the same region as ORF 575R in Ehime-1, encodes a myristoylated membrane protein, known as a viral envelope membrane protein of iridovirus, and its function may be conserved throughout the Iridoviridae (Zhou *et al.*, 2011). Thus, an InDel in the coding region of a viral membrane protein (a 30 bp deletion in ORF 101R of 17RbGs) may alter the regulation of viral entry into the host cell at the onset of the infection cycle.

Moreover, this study elucidates the virulence of RSIVs (17SbTy as RSIV mixed subtype I/II and 17RbGs as RSIV subtype II) in rock bream, which is known as one of the most susceptible hosts for RSIVD. The virulence of two RSIV isolates (17SbTy as RSIV mixed subtype I/II and 17RbGs as RSIV subtype II), which genetically differ, was analyzed by viral replication in rock bream cells (*in vitro*), correlation of mortality, and viral and apoptosis-related gene expression in rock bream (*in vivo*).

From the viral culture, even though the genome copy number of extracellular RSIV released from two isolate-infected RBF cells increased after 3 dpi, viral genome copy numbers of 17RbGs were significantly higher (approximately 10-fold difference) than those of 17SbTy (Figure 6), suggesting the infectivity difference between the two RSIV isolates. In addition, this result indicated that genetic mutations, such as InDels in genes encoding myristoylated membranes and DNA binding proteins, could be related to viral replication in rock bream cells.

In the challenging test, no 17RbGs infected rock bream survived at 14 dpi, whereas 28.6% (6/21) of 17SbTy infected rock bream were survived at 21 dpi (Figure 7), and

the difference in survival rates of two RSIVs against rock bream was significantly different (log-rank test, $P < 0.05$). These results suggest that several of the genetic factors identified during the genomic characterization, including the InDels in coding regions, may influence virulence. Another noteworthy observation is that the apparent difference in virulence between the RSIV isolates may be due to adaptations to their respective original hosts (the Japanese seabass for 17SbTy and the rock bream for 17RbGs).

The viral shedding ratio is a major factor in evaluating viral transmission and its risk (Wargo *et al.*, 2017; Kawato *et al.*, 2021). In this study, based on the viral genome copy numbers in the host and rearing water, the viral shedding ratios of the RSIV isolates were compared. The maximum number of viral genome copies in the host and rearing water was determined at 11 and 14 days after RSIV-IP injection, suggesting that the virus released from the host in the environment could rise to the maximum levels after a period of infection, similar to other aquatic animal viruses (Molloy *et al.*, 2014; Kim *et al.*, 2017). In addition, different maximum amounts for viral shedding ratio after 17SbTy and 17RbGs infection were identified as 1.23×10^5 and 7.76×10^5 viral genome copies number/L/g at 14 days, respectively (Figure 8). Although it was difficult to evaluate the infectivity of seawater concentrates in vitro and in vivo because of their low stability to resuspension in EDTA-containing chemicals required in the seawater concentration process (Poulos *et al.*, 2018), there was a clear difference in the viral shedding ratio of the two RSIVs.

A variety of previous studies regarding RSIV pathogenicity (Kawato *et al.*, 2021; Sumithra *et al.*, 2022) have focused on the mortality of the host, viral genomic copy numbers in tissue, and clinical signs without risk evaluation based on the odds ratio. The odds ratio is one of the major statistical methods for the risk assessment of the relationship between infection and clinical signs (Zhang *et al.*, 1998). Thus, clinical signs may play a crucial role in the evaluation of the relative risk of pathogens. The general behaviour of infected fish is abnormal swimming and lethargy (Wang *et al.*, 2003; Subramaniam *et al.*, 2012). In addition, these fish showed enlarged spleens caused by hypertrophic cells, supporting the use of the spleen index as a clinical index for RSIVD (Jin *et al.*, 2011; Jung *et al.*, 2019). In this study, based on three clinical factors for RSIVD, including spleen index, abnormal swimming, and lethargy, the relative pathogenic risk of RSIV isolates was evaluated (Table 6). Notably, the odds ratio through spleen index overvalues by 17RbGs infection was 55.00, a significantly different finding in 17SbTy infection (19.38). As previously mentioned by Jung *et al.*, 2019, the spleen index was correlated with mortality and viral genome copy number and was suggested as an indicator of RSIV virulence. The odds ratio based on the spleen index could also be used as an indicator for RSIV virulence supported by their pathogenicity to rock bream.

To identify viral transmission under natural mimic conditions, cohabitation between RSIV-infected (donor) and naïve (recipient) rock bream was conducted as previously described (Min *et al.*, 2021). Ten days after infection, the first mortality of the donor fish was observed, and every recipient fish showed mortality caused by clinical

infection with the released virus from the donor fish and/or the transmitted virus itself (Figure 9). At different injection doses for the donor, cumulative mortality in the 17RbGs-donor (100.0% at high and 80.0% at low doses) was different from that of the 17SbTy-donor (53.33% at high and 33.33% at low doses), supporting the relationship between genetic mutation and pathogenicity for the 17SbTy isolate as a low pathogenic RSIV (Figure 9). Regardless of the injected RSIV dose (high and low) to donor fish, recipient fish in the 17RbGs group (86.67% at high dose and 80.0% at low dose) showed significantly different mortality rates compared with those in the 17SbTy group (46.67% at high dose, 33.33% at low dose). Thus, the result of the cohabitation challenge suggests that viral transmission after infection with RSIV mixed subtype I/II (17SbTy isolate) may have a lower relative transmission risk than infection with general RSIV subtype II (17RbGs isolate) in a natural environment. Furthermore, the viral shedding ratio described above supports the possibility of reinfection through the transmitted recipient from donor-dependent RSIV infectivity in the cohabitation experiments.

Virulence is defined as pathogenicity and could differ depending on the host-pathogen interaction (Casadevall *et al.*, 1999). Thus, to elucidate the virulence difference between RSIV, a study on host-pathogen interactions should be conducted. In this study, viral genes as well as apoptosis-related genes, suggesting one of the virulence factors for RSIV infection (Imajoh *et al.*, 2004; He *et al.*, 2006), were analyzed. From the analysis of viral gene expression, polymerase and major capsid protein genes representing viral replication were upregulated, with differential

expression between RSIV isolates at 11 days post-injection (Figure 10A). DNA-binding proteins and myristoylated membrane proteins were suggested as remarkable genetic variant regions (InDels) compared with RSIV isolates (17SbTy and 17RbGs) (Figure 5A and D). Moreover, these genes were upregulated at different levels in infected rock bream (Figure 10A), supporting that the genetic variation could be related to their pathogenicity. The difference in virus titer between the two isolates might be affect the expression of apoptosis-related genes (Figure 8 and 10B). Furthermore, the host could induce apoptosis associated with the limitation of viral replication (Everett *et al.*, 1999), even in some viruses, such as RSIV, which could also induce apoptosis via caspase pathways (Imajoh *et al.*, 2004). Thus, the induction of caspase-dependent apoptosis in the early stages of viral infection affects to RSIV replication clearly related to pathogenicity (Imajoh *et al.*, 2004; Jung *et al.*, 2014). Caspase-dependent apoptosis can be activated by caspase-8 and -9, as well as by the caspase-3 pathway (Dockrell *et al.*, 2001; Chen *et al.*, 2009; Imajoh *et al.*, 2004). In addition, rock bream PDCD10, a cytoskeleton and cellular adaptor protein, participates in apoptosis through the caspase-3 pathway (Chen *et al.*, 2009; Kim *et al.*, 2016).

From the comparative results of apoptosis-related gene expression between 17SbTy and 17RbGs infection, caspase-8 genes were significantly upregulated compared to that in the control group (Figure 10B). Interestingly, the upregulation of caspase-8 gene expression was significantly different at 11 days post-injection between the two RSIVs, similarly to viral gene expression (Figure 10). Notably, the difference in caspase-8 gene expression may be related to the difference in the early stages of viral replication

between 17SbTy and 17RbGs (Figure 10). Caspase-8, by activation of the death receptor-mediated pathway, can induce a caspase cascade including caspase-3 (Schmitz *et al.*, 2000; Krueger *et al.*, 2001; Henderson *et al.*, 2002), suggesting that caspases-8 can be played a role as an initial regulating factor for caspase-dependent apoptosis by RSIV infection. In contrast to caspase-8 gene expression, although caspase-3 and PDCD10 were upregulated by RSIV infection, these levels were not significantly different during the experimental period (11 days, as before showing rock bream death by RSIV infection) (Figure 10B). Similarly, in the other study (Jung *et al.*, 2014), caspase-3 expression was not significantly upregulated compared to that in the control group, suggesting that apoptosis was inhibited during rock bream iridovirus (RBIV; RSIV-type) infection. In addition, although caspase-8 was upregulated, apoptosis inhibition by low caspase-3 gene expression levels may lead to an increased number of RBIV-infected cells in rock bream (Jung *et al.*, 2014). In addition, although caspase-8 was upregulated, apoptosis inhibition by low caspase-3 gene expression levels may lead to an increased number of RBIV-infected cells in rock bream (Jung *et al.*, 2014). Thus, it suggested that 17SbTy and 17RbGs might be shared this function which is apoptosis inhibition of rock bream and is supported that different expression levels of viral genes between 17RbGs and 17SbTy isolates in the early infection stage lead to differences in apoptosis inhibition and pathogenicity (mortality for rock bream). These results indicate that the viral and caspase-8 genes can be used to detect differences in virulence between RSIV isolates.

In conclusion, this study elucidated previously unassessed complete genomic characteristics and virulence traits between RSIV subtype II (17RbGs) and novel mixed subtype I/II (17SbTy) viruses, which showed genetic differences. From the complete genome analysis, two RSIV isolates (17SbTy, 112,360 bp; 17RbGs, 112,360 bp) have the genomic organization, G+C content, coding capacity, and conserved core genes typical of the RSIV. Notably, the best matches for the nucleotide sequences in the 115 ORFs of 17SbTy are RSIV subtype II (69 matching ORFs; 97.48%–100% identity) and RSIV subtype I (46 matching ORFs; 98.77%–100% identity). In comparison with RSIVs, 17SbTy and 17RbGs have remarkable InDels in regions (ORFs 014R and 102R based on the 17SbTy) encoding a DNA-binding protein and myristoylated membrane protein, respectively. In addition, these RSIVs with genetic differences also showed critical differences in survival rates in rock bream (17RbGs was more pernicious to rock bream than 17SbTy). And additional driving factors for virulence determinants were considered such as viral shedding and odds ratio after RSIV infection in rock bream, supporting the 17SbTy isolate (RSIV mixed subtype I/II) was relatively less pathogenic RSIV than 17RbGs (RSIV subtype II). In particular, as well as the odds ratio based on the spleen index, as one of the mechanisms of pathogen-host interactions, high expression levels of viral genes in the early stage of infection with 17RbGs may induce apoptosis inhibition, supporting the virulence differences between RSIV isolates. Furthurmore, although 17SbTy showed relatively low pathogenicity than 17RbGs in rock bream (*Oplegnathus fasciatus*), it is also necessary to evaluate virulence in Japanese seabass (*Lateolabrax japonicas*). Thus, the complete genome sequences of

these RSIV isolates provide basic information for molecular epidemiology and the virulence assessment through various approaches for virulence determinants provides insights into the prediction and comparison of virulence among RSIVs.

SUMMARY

The causative agents of red sea bream iridoviral disease (RSIVD) are known as infectious spleen and kidney necrosis virus (ISKNV) and red sea bream iridovirus (RSIV). In Korea, RSIV, especially subtype II, has been the main causative agent of red sea bream iridoviral disease since the 1990s. Recently, RSIV-Ku strain, a novel strain mixed with ISKNV and RSIV, was isolated from cultured red sea bream (*Pagrus major*) in Taiwan, suggesting the possibility of genetic variation in the aquatic environment.

In this study, RSIV infection was identified in Japanese sea bass (*Lateolabrax japonicus*) and rock bream (*Oplegnathus fasciatus*) among Korean cultured fish, and the two RSIV isolates were had different subtypes on the phylogenetic analysis based on the major capsid protein (MCP) and the adenosine triphosphatase (ATPase) protein genes. The complete genome and pathogenicity were analyzed to find out the differences between 17SbTy (RSIV mixed subtype I/II isolated from the Japanese sea bass) and 17RbGs (RSIV subtype II isolated from the rock bream).

Complete genome sequences revealed that 17SbTy and 17RbGs genomes are 112,360 and 112,235 bp long, respectively (115 and 114 open reading frames [ORFs], respectively). According to nucleotide sequence homology with representative RSIVs, 69 of 115 ORFs of 17SbTy are most closely related to subtype II (98.48–100% identity), and 46 to subtype I (98.77–100% identity). In addition, two isolated RSIVs in this study

compared genetic variants with Ehime-1 strain (RSIV subtype I) reported in Japan and RBIV strain (RBIV subtype II) in Korea. As the result, RSIV subtype I/II (17SbTy isolate) and RSIV subtype II (17RbGs isolate) carried two insertion/deletion mutations (InDels) (ORFs 014R and 102R on the basis of the 17SbTy) in regions encoding functional proteins (a DNA-binding protein and a myristoylated membrane protein).

The survival rates of RSIV subtype I/II (17SbTy isolate) or RSIV subtype II (17RbGs isolate) infected rock bream differed significantly. It indicated that the genomic characteristics and/or adaptations to their respective original hosts might influence pathogenicity. The transmission assessment based on the maximum RSIV shedding ratio of inoculated rock bream suggested that the RSIV subtype I/II could have a relatively lower risk than that of infection with RSIV subtype II. In addition, the analysis of the odds ratio based on the spleen index indicated a significantly different that RSIV subtype II infected rock bream was 19.38 but RSIV subtype II was 55.00, supporting the virulence difference of RSIV isolates to rock bream. Especially, in a cohabitation challenge test that mimicked natural conditions, the cumulative mortality of the donor (RSIV-injected rock bream) and the recipient (cohabited naïve rock bream) was significantly lower in the RSIV subtype I/II exposed group than RSIV subtype II exposed group, supporting the correlation between genetic mutation and pathogenicity.

To identify the infection mechanism of two RSIVs which has differences in pathogenicity to rock bream and genetic characteristics, the expression of the viral and apoptosis-related genes were analyzed after RSIVs inoculation to rock bream. The

expressions of the viral gene (DNA binding protein and myristoylated membrane protein) including the notable InDels region and that of caspase-8 related to apoptosis in rock bream were up-regulated with significantly differences between two RSIVs infected rock bream at 11 days post-infection. It might be related to the difference of viral replication between 17SbTy and 17RbGs in the early stages. Furthermore, although viral genes were highly expressed and caspase-8 was upregulated in early infection stages, the low expression of caspase-3 (activated by caspase-8) may have inhibited apoptosis, reflecting differences in virulence between different RSIV isolates.

In conclusion, several virulence factors, including pathogenicity, viral shedding ratio, odds ratio, and gene expression in genetic different RSIV (RSIV subtype I/II and RSIV subtype II) infected rock bream, support that RSIV mixed subtype I/II may be a less pathogenic RSIV strain compared with general RSIV subtype II in a natural aquatic environment.

ACKNOWLEDGEMENTS

새로운 환경에서 새로운 시작이었기에, 두려움, 그리고 설렘이 함께 출발했던 대학원 생활이 벌써 2 년이 흘러 이 논문과 함께 마무리되고 있습니다. 본 논문이 결실을 맺기까지 참 많은 분들의 도움이 있었습니다. 그분들께 이 글을 통해 감사의 마음을 전하고자 합니다.

본 논문을 완성하기까지 저를 많은 격려와 가르침으로 이끌어 주신 존경하는 김광일 지도 교수님께 깊은 감사의 마음을 드립니다. 교수님 지도 아래 감히 처음으로 졸업하는 제자가 되었습니다. 이러한 영광을 갖게 되어 너무 자랑스럽습니다. 그리고 어깨가 무겁습니다. 그렇기에 어디에서도 초심을 잃지 않고, 교수님처럼 섬세하고, 성실하고, 또 존경받는 사람이 되기 위해 노력하겠습니다. 그리고 바쁘신 와중에 본 논문에 관심을 가져주시고 논문의 질적 향상을 위해 조언과 지도를 해주신 김기홍 교수님, 김도형 교수님께 감사드립니다. 타대학 학부 과정을 졸업하여 부족한 저에게 석사 과정 동안 많은 가르침 주신 정현도 교수님, 정준기 교수님, 강주찬 교수님, 허민도 교수님께 감사드립니다.

대학원 생활을 함께한 진단생화학실험실 선배님, 동기, 후배님들께 고마운 마음을 전합니다. 석사 과정을 통해 대학원생으로서 처음 만난 민준규 선배님, 예진이에게 고맙다는 말을 전하고 싶습니다. 동기로 친구로 많은 힘과 격려가 되어준 예진이에게 먼저 실험실을 마무리하게

되어 미안한 마음과 그동안 함께했던 추억과 위로와 격려에 설명할 수 없는 고마운 마음을 응원과 함께 전합니다. 학위 과정동안 실험 뿐만 아니라 희로애락을 함께했던 국현, 희주, 민재, 은진, 소원, 원준, 지영이에게 고마운 마음을 전합니다. 그리고 앞으로 실험실을 화사하게 꽃피울 유경, 윤정, 동준, 이설, 나경, 민경, 소영이에게도 기대와 고마운 마음을 전합니다. 또, 부족한 선배지만 졸업까지 믿고 따라준 혜원, 지수, 은빈, 은채에게도 고마운 마음과 각자의 미래에 대한 응원을 전합니다.

다른 실험실이고, 타 대학 학부를 마치고 온 낯선 후배에게 친절하고 따뜻하게 맞아주신 부경대학교 수산생명의학과 모든 선후배님들께 이 기회를 통해 감사의 마음을 전합니다.

우리 가족, 어머니, 아버지께서 항상 저의 선택에 무한한 믿음과 영원한 지지가 되어주시기에 좀 더 자유롭고, 세상을 따뜻한 마음으로 바라볼 수 있는 사람이 될 수 있었다고 생각합니다. 그저 지식인이 아닌 지혜로운 사람이 되어 세상에 이바지할 수 있는 사람이 되겠습니다. 감사합니다. 가장 가까이에서 나의 대학부터 대학원 생활을 공감하고 격려해준 진아 언니에게 덕분에 해낼 수 있었다고 고마운 마음을 전합니다. 또, 학생으로서 자신의 꿈을 향해 다가가고 있는 내 동생, 세현이에게도 고마운 마음과 응원을 드립니다.

석사 과정을 마무리하며 올해 봄, 커리어에 또 하나의 큰 선택의 순간이 있었습니다. 저의 미래를 함께 고민해주시고, 지지해주신 김광일 교수님과 정현도 교수님, 그리고 우진비앤지㈜ 김정한 이사님, 서병주 부장님, 권우주 과장님께 다시 한번 깊은 감사의 말씀을 드리며 마칩니다. 이제 저도 사회에 나가 구성원으로서 저의 역할을 잘 해내는 여러분들의 자랑스러운 제자, 그리고 사람이 되겠습니다. 2022 년 여름, 저의 스물 일곱살을 함께 해주셔서 감사합니다.

REFERENCES

Andrews, S., 2010, Babraham bioinformatics-FastQC a quality control tool for high throughput sequence data. *URL: https://www. bioinformatics. babraham. ac. uk/projects/fastqc*.

Casadevall, A., Pirofski, L.A., 1999, Host-pathogen interactions: redefining the basic concepts of virulence and pathogenicity, *Infect Immun.* 67 (8), 3703-3713.

Chen, L., Tanriover, G., Yano, H., Friedlander, R., Louvi, A., Gunel, M., 2009, Apoptotic functions of PDCD10/CCM3, the gene mutated in cerebral cavernous malformation 3, *Stroke*. 40 (4), 1474-1481.

Chinchar, V.G., Hick, P., Ince, I.A., Jancovich, J.K., Marschang, R., Qin, Q., Subramaniam, K.; Waltzek, T.B.; Whittington, R.; Williams, T.; Zhang, Q.Y., 2017, ICTV virus taxonomy profile: *Iridoviridae*. *J. Gen. Virol.* 98, 890–891.

Do, J.W., Moon, C.H., Kim, H.J., Ko, M.S., Kim, S.B., Son, J.H., Park, J.W., 2004, Complete genomic DNA sequence of rock bream iridovirus. *Virology*. *325*, 351–363.

Do, J.W., Cha, S.J., Kim, J.S., An, E.J., Lee, N.S., Choi, H.J., Lee, C.H., Park, M.S., Kim, J.W., Kim, Y.C., Park, J.W. Phylogenetic analysis of the major capsid

protein gene of iridovirus isolates from cultured flounders *Paralichthys olivaceus* in Korea. *Dis. Aquat. Organ.* 2005, *64*, 193–200.

Dockrell, D.H. 2001, Apoptotic cell death in the pathogenesis of infectious diseases, *J Infect.* 42, 227-234.

Eaton, H.E., Metcalf, J., Penny, E., Tcherepanov, V., Upton, C., Brunetti, C.R., 2007, Comparative genomic analysis of the family *Iridoviridae*: re-annotating and defining the core set of iridovirus genes. *Virol. J. 4*, 1–17.

Eaton, H.E., Ring, B.A., Brunetti, C.R., 2010, The genomic diversity and phylogenetic relationship in the family *Iridoviridae*. *Viruses*. *2*, 1458–1475.

Elvitigala, D.A.S., Whang, I., Premachandra, H.K.A., Umasuthan, N., Oh, M.J., Jung, S.J., Lee, J., 2012, Caspase 3 from rock bream (*Oplegnathus fasciatus*): genomic characterization and transcriptional profiling upon bacterial and viral inductions, *Fish Shellfish Immunol.* 33 (1), 99-110.

Everett, H., McFadden, G., 1999, Apoptosis: an innate immune response to virus infection, *Trends Microbiol*. 7 (4), 160-165.Oh, M.J., Jung, S.J., Kim, Y.J., 1999,Detection of RSIV (red sea bream iridovirus) in the cultured marine fish by the polymerase chain reaction. *Fish Pathol. 12*, 66–69.

Ewels, P., Magnusson, M., Lundin, S., Käller, M., 2016, MultiQC: summarize analysis results for multiple tools and samples in a single report. *Bioinformatics*. *32*,

3047–3048.

Fusianto, C.K., 2021, Detection and control of Infectious spleen and kidney necrosis virus in aquaculture, *The University of Sydney (Doctoral dissertation)*.

Galperin, M. Y., Makarova, K. S., Wolf, Y. I., Koonin, E. V., 2015, Expanded microbial genome coverage and improved protein family annotation in the COG database. *Nucleic acids research*. 43(D1), D261-D269.

Go, J., Whittington, R., 2019, Australian bass Macquaria novemaculeata susceptibility to experimental megalocytivirus infection and utility as a model disease vector, *Dis Aquat Organ*. 133 (2), 157-174.

Grant J.R., Arantes A.S., Stothard P., 2012, Comparing thousands of circular genomes using the CGView Comparison Tool. *BMC Genom. 13*, 1–8.

Hackl, T., Hedrich, R., Schultz, J., Förster, F., 2014, proovread: large-scale high-accuracy PacBio correction through iterative short read consensus. *Bioinformatics*. *30*, 3004–3011.

He, J.G., Deng, M., Weng, S.P., Li, Z., Zhou, S.Y., Long, Q.X., Chan, S.M., 2001, Complete genome analysis of the mandarin fish infectious spleen and kidney necrosis iridovirus. *Virology*. *291*, 126–139.

He, J.G., Zeng, K., Weng, S.P., Chan, S.M., 2002, Experimental transmission,

pathogenicity and physical-chemical properties of infectious spleen and kidney necrosis virus (ISKNV), *Aquaculture*. 204, 11–24.

He, W., Yin, Z.X., Li, Y., Huo, W.L., Guan, H.J., Weng, S.P., He, J.G., 2006, Differential gene expression profile in spleen of the mandarin fish *Siniperca chuatsi* infected with ISKNV, derived from suppression subtractive hybridization, *Dis Aquatic Organ.* 73 (2), 113-122.

Henderson, G., Peng, W., Jin, L., Perng, G.C., Nesburn, A.B., Wechsler, S.L., Jones, C., 2002, Regulation of caspase 8–and caspase 9–induced apoptosis by the herpes simplex virus type 1 latency-associated transcript. *J Neurovirol. 8*, 103-111.

Hong, S., Jin, J.W., Park, J.H., Kim, J.K., Jeong, H.D., 2016, Analysis of proinflammatory gene expression by RBIV infection in rock bream, Oplegnathus faciatus, *Fish Shellfish Immunol.*, 50, 317-326.

Imajoh, M., Sugiura, H., Oshima, S.I., 2004, Morphological changes contribute to apoptotic cell death and are affected by caspase-3 and caspase-6 inhibitors during red sea bream iridovirus permissive replication, *Virology*. 322 (2), 220-230.

Inouye, K., Yamano, K., Maeno, Y., Nakajima, K., Matsuoka, M., Wada, Y., Sorimachi, M., 1992, Iridovirus infection of cultured red sea bream, *Pagrus*

major. *Fish. Pathol*. *27*, 19–27.

Jeong, J.B., Jun, J.L., Yoo, M.H., Kim, M.S., Komisar, J.L., Jeong, H.D., 2003, Characterization of the DNA nucleotide sequences in the genome of red sea bream iridoviruses isolated in Korea. *Aquaculture. 220*, 119–133.

Jeong, Y.J., Kim, Y.C., Min, J.G. Jeong, M.A. Kim, K.I., 2021, Characterization of rock bream (*Oplegnathus fasciatus*) fin cells and its susceptibility to different genotypes of megalocytiviruses. *Fish Pathol*., 34 (2), 149-159.

Jin, J.W., Cho, H.J., Kim, K.I., Jeong, J.B., Park, G.H., Jeong, H.D., 2011, Quantitative analysis of the clinical signs in marine fish induced by Megalocytivirus infection, *Fish Pathol.* 24 (2), 53-64.

Jin, J.W., Kim, Y.K., Hong, S., Kim, Y.C., Kwon, W.J., Jeong, H.D., 2018, Identification and characterization of Megalocytivirus type 3 infection with low mortality in starry flounder, Platichthys stellatus, in Korea, *J World Aquac Soc*. 49 (1), 229-239.

John, S.G., Mendez, C.B., Deng, L., Poulos B., Kauffman, A.K., Kern, S., Brum, J., Polz, M.F., Boyle, E.A., Sullivan, M.B., 2011, A simple and efficient method for concentration of ocean viruses by chemical flocculation, *Environ Microbiol Rep.* 3.2, 195-202.

Jung, M.H., 2012, Analysis of MHC polymorphism and immune genes expression

to iridovirus infection in rock bream, *Chonnam National University (Doctoral dissertation)*.

Jung, M.H., Jung, S.J., 2019, Correlation of virus replication and spleen index in rock bream iridovirus infected rock bream *Oplegnathus fasciatus*, *Fish Pathol*. 32 (1), 1-8.

Jung, M.H., Nikapitiya, C., Song, J.Y., Lee, J.H., Lee, J., Oh, M.J., Jung, S.J., 2014, Gene expression of pro-and anti-apoptotic proteins in rock bream

(*Oplegnathus fasciatus*) infected with megalocytivirus (family *Iridoviridae*). *Fish Shellfish Immunol.* 37 (1), 122-130.

Jung, S.J., Oh, M.J., 2000, Iridovirus-like infection associated with high mortalities of striped beakperch, *Oplegnathus fasciatus* (Temminck et Schlegel), in southern coastal areas of the Korean peninsula, *J Fish Dis*. 23 (3), 223-226.

Kawakami, H., Nakajima, K., 2002, Cultured fish species affected by red sea bream iridoviral disease from 1996 to 2000. *Fish Pathol. 37*, 45–47.

Kawato, Y., Ito, T., Kamaishi, T., Fujiwara, A., Ototake, M., Nakai, T., Nakajima, K., 2016, Development of red sea bream iridovirus concentration method in seawater by iron flocculation. *Aquaculture.* 450, 308-312.

Kawato, Y., Subramaniam, K., Nakajima, K., Waltzek, T., Whittington, R., 2017,

Iridoviral diseases: red sea bream iridovirus and white sturgeon iridovirus, In Woo PTK, Cipriano RC (Eds.), Fish viruses and bacteria: pathobiology and protection. *CABI Publishing*, Wallingford, UK. 147–159.

Kawato, Y., Mekata, T., Inada, M., Ito, T., 2021, Application of environmental DNA for monitoring red sea bream iridovirus at a fish farm, *Microbiol. Spectr.* e00796-21.

Kim, G.H., Kim, M.J., Choi, H.J., Koo, M.J., Kim, M.J., Min, J.G, Kim, K.I., 2021, Evaluation of a novel TaqMan probe-based real-time PCR assay for detection and quantification of red sea bream iridovirus. *Fish Aquat Sci*. *24*, 351–359.

Kim, J.W., Jeong, J.M., Bae, J.S., Cho, D.H., Jung, S.H., Hwang, J.Y., Kwon, M.G., Seo, J.S., Baeck, G.W., Park, C.I., 2016, First description of programmed cell death10 (PDCD10) in rock bream (*Oplegnathus fasciatus*): Potential relations to the regulation of apoptosis by several pathogens. *Dev Comp Immunol.* 55, 51-55.

Kim, K.I., Kim, Y.C., Kwon, W.J, Jeong, H.D, 2017, Evaluation of blue mussel *Mytilus edulis* as vector for viral hemorrhagic septicemia virus (VHSV), *Dis Aquat Organ.* 126 (3), 239-246.

Kim, K.I., Hwang, S.D., Cho, M.Y., Jung, S.H., Kim, Y.C., Jeong, H.D., 2018, A

natural infection by the red sea bream iridovirus-type Megalocytivirus in the golden mandarin fish Siniperca scherzeri. *J. Fish. Dis*. 41, 1229–1233.

Kim, K.I., Lee, E.S., Do, J.W., Hwang, S.D., Cho, M., Jung, S.H., Jee, B.Y., Kwon, W.J., Jeong, H.D., 2019, Genetic diversity of *Meglaocytivirus* from cultured fish in Korea. *Aquaculture. 509*, 16–22.

Krueger, A., Baumann, S., Krammer, P.H., Kirchhoff, S., 2001, FLICE-inhibitory proteins: regulators of death receptor-mediated apoptosis, *Mol Cell Biol.* 21 (24) 8247-8254.

Kurita, J., Nakajima, K., Hirono, I., Aoki, T., 1998, Polymerase chain reaction (PCR) amplification of DNA of red sea bream iridovirus (RSIV). *Fish Pathol. 33*, 17–23.

Kurita, J., Nakajima, K., Hirono, I., Aoki, T., 2002, Complete genome sequencing of red sea bream iridovirus (RSIV). *Fish. Sci. 68*, 1113–1115.

Kurita, J., Nakajima, K., 2012, Megalocytiviruses. *Viruses. 4*, 521–538.

Min, J.G., Jeong, Y.J., Jeong, M.A., Kim, J.O., Hwang, J.Y., Kwon, M.G., Kim, K.I., 2021, Experimental transmission of red sea bream iridovirus (RSIV) between rock bream (*Oplegnathus fasciatus*) and rockfish (*Sebastes schlegelii*), *Fish Pathol*. 34 (1), 1-7.

Molloy, S.D., Pietrak, M.R., Bouchard, D.A., Bricknell, I., 2014, The interaction of infectious salmon anaemia virus (ISAV) with the blue mussel, *Mytilus edulis*. Aquac Res., 45, 509-518.

OIE (World Organisation for Animal Health), 2021, Manual of Diagnostic Tests for Aquatic Animal.

Orzalli, M.H., Kagan, J.C., 2017, Apoptosis and necroptosis as host defense strategies to prevent viral infection, *Trends Cell Biol*. 27 (11), 800-809.

Poulos, B.T., John S.G., Sullivan M.B., 2018, Iron chloride flocculation of bacteriophages from seawater, *Bacteriophage*. Chapter 4, Humana Press, New York, 49-57.

Schmitz, I., Kirchhoff, S., Krammer, P.H., 2000, Regulation of death receptor-mediated apoptosis pathways, *Int J Biochem Cell Biol.* 32 (11-12), 1123-1136.

Shi, C. Y., Jia, K. T., Yang, B., Huang, J., 2010, Complete genome sequence of a Megalocytivirus (family *Iridoviridae*) associated with turbot mortality in China. *Virol. J. 7*, 1–9.

Shiu, J.Y., Hong, J.R., Ku, C.C., Wen, C.M. Complete genome sequence and phylogenetic analysis of megalocytivirus RSIV-Ku: A natural recombination infectious spleen and kidney necrosis virus. *Arch. Virol.*

2018, *163*, 1037–1042.

Subramaniam, K., Shariff, M., Omar, A.R., Hair-Bejo, M., 2012, *Megalocytivirus* infection in fish. *Rev. Aquac.* 4 (4), 221-233.

Sumithra, T.G., Sharma, S.K., Neelima, L., Dhanutha, N.R., Joshy, A., Anusree V.N., Rajesh K.M., 2022, Red sea bream iridovirus infection in cage farmed Asian sea bass (*Lates calcarifer*): Insights into the pathology, epizootiology, and genetic diversity, *Aquaculture*. 548, 737571.

Tatusov, R.L., Koonin, E.V., Lipman, D.J. 1997, A genomic perspective on protein families. *Science*. 278, 631–637.

Tatusov,R.L., Natale,D.A., Garkavtsev, I.V., Tatusova,T.A., Shankavaram,U.T., Rao, B.S., Kiryutin, B., Galperin, M.Y., Fedorova, N.D., Koonin, E.V., 2001, The COG database: new developments in phylogenetic classification of proteins from complete genomes. *Nucleic Acids Res*. *29*, 22–28.

Tompkins, D.M., Carver, S., Jones, M.E., Krkošek, M., Skerratt, L.F., 2015, Emerging infectious diseases of wildlife: a critical perspective, *Trends Parasitol.* 31 (4), 149-159.

Wang, C.S., Shih, H.H., Ku, C.C., Chen, S.N., 2003, Studies on epizootic iridovirus infection among red sea bream, *Pagrus major* (Temminck & Schlegel), cultured in Taiwan, *J Fish Dis.,* 26 (3), 127-133.

Wargo, A.R., Scott, R.J., Kerr, B., Kurath, G., 2017, Replication and shedding kinetics of infectious hematopoietic necrosis virus in juvenile rainbow trout, *Virus Res.* 227, 200-211.

Xiang, Z., Weng, S., Qi, H., He, J., Dong, C., 2014, Identification and characterization of a novel FstK-like protein from spotted knifejaw iridovirus (genus *Megalocytivirus*). *Gene*. 545, 233–240.

Zhang, B. C., Zhang, M., Sun, B. G., Fang, Y., Xiao, Z. Z., Sun, L., 2013, Complete genome sequence and transcription profiles of the rock bream iridovirus RBIV-C1. *Diseases of aquatic organisms*. 104(3), 203-214.

Zhang, J., Kai, F.Y., 1998, What's the relative risk?: A method of correcting the odds ratio in cohort studies of common outcomes. *Jama*. 280 (19), 1690-1691.

Zhou, S., Wan, Q., Huang, Y., Huang, X., Cao, J., Ye, L., Qin, Q., 2011, Proteomic analysis of Singapore grouper iridovirus envelope proteins and characterization of a novel envelope protein VP088. *Proteomics*. *11*, 2236–22